Review: Periodate oxidation of wood polysaccharides—Modulation of hierarchies

Downloaded from: https://research.chalmers.se, 2025-12-04 23:27 UTC

Citation for the original published paper (version of record):
Nypelö, T., Berke, B., Spirk, S. et al (2021). Review: Periodate oxidation of wood polysaccharides—Modulation of hierarchies. Carbohydrate Polymers, 252. http://dx.doi.org/10.1016/j.carbpol.2020.117105

N.B. When citing this work, cite the original published paper.

research.chalmers.se offers the possibility of retrieving research publications produced at Chalmers University of Technology. It covers all kind of research output: articles, dissertations, conference papers, reports etc. since 2004. research.chalmers.se is administrated and maintained by Chalmers Library

(article starts on next page)

Carbohydrate Polymers 252 (2021) 117105

Contents lists available at ScienceDirect

Carbohydrate Polymers

journal homepage: www.elsevier.com/locate/carbpol

Review

Review: Periodate oxidation of wood polysaccharides—Modulation of hierarchies

Tiina Nypelö [a,b,*], Barbara Berke [c], Stefan Spirk [d], Juho Antti Sirviö [e]

[a] Department of Chemistry and Chemical Engineering, Chalmers University of Technology, Gothenburg, Sweden
[b] Wallenberg Wood Science Center, Chalmers University of Technology, Gothenburg, Sweden
[c] Department of Physics, Chalmers University of Technology, Gothenburg, Sweden
[d] Institute of Bioproducts and Paper Technology, Graz University of Technology, Graz, Austria
[e] Fibre and Particle Engineering Research Unit, University of Oulu, Oulu, Finland

ARTICLE INFO

Keywords:
Periodate oxidation
Cellulose
Hemicellulose
Cellulose fibres
Cellulose fibrils
Cellulose nanocrystals

ABSTRACT

Periodate oxidation of polysaccharides has transitioned from structural analysis into a modification method for engineered materials. This review summarizes the research on this topic. Fibers, fibrils, crystals, and molecules originating from forests that have been subjected to periodate oxidation can be crosslinked with other entities via the generated aldehyde functionality, that can also be oxidized or reduced to carboxyl or alcohol functionality or used as a starting point for further modification. Periodate-oxidized materials can be subjected to thermal transitions that differ from the native cellulose. Oxidation of polysaccharides originating from forests often features oxidation of structures rather than liberated molecules. This leads to changes in macro, micro, and supramolecular assemblies and consequently to alterations in physical properties. This review focuses on these aspects of the modulation of structural hierarchies due to periodate oxidation.

1. Introduction

This review focuses on the structural changes that wood polysaccharide materials undergo during periodate oxidation. In the context of engineering materials from wood resources, periodate oxidation is currently of interest, since it is a way of modulating physical and chemical properties of materials with an oxidation reaction in aqueous conditions. The purpose of this review is to present the current state of the research and to support future research endeavors.

The recent emergence of the structural impacts of periodate oxidation on polysaccharide materials comes as a natural progression of the copious research on the oxidation reaction. Periodate oxidation of polysaccharides (Malaprade, 1928) has historically been employed for polysaccharide molecular analysis (Abdel-Akher, Hamilton, Montgomery, & Smith, 1952; Aspinall & Ross, 1963; Bobbitt, 1956; Guthrie, 1962). Mild oxidation conditions are easy to apply to polysaccharides, as selective cleavage of the pyranose ring combined with acid hydrolysis to split the acyclic acetal linkages enables the detection of mono-/-oligomers [e.g. Smith degradation reaction (Abdel-Akher et al., 1952)] and their backtracking to the initial structure. The periodate oxidation reaction and many of the molecular properties of oxidized moieties are well understood. Freshly oxidized aldehyde groups can transfer into hydrated forms, form hemiacetal/hemialdal linkages with hydroxyl groups in proximity, or link to other moieties, such as amine-containing species.

Mechanistic reaction considerations are outside the scope of this review, and the reader is referred to original research contributions [e.g., Varma and Kulkarni (2002)], recent reviews (Khalil et al., 2014; Nechyporchuk, Belgacem, & Bras, 2016), and books [e.g. Dryhurst (2015)]. This includes the oxidation of xylan (Heinze, Koschella, & Ebringerova, 2004) and polymeric properties of oxidized polysaccharides (Kristiansen, Potthast, & Christensen, 2010). We recommend the groundbreaking works of Bobbitt (1956), Abdel-Akher et al. (1952), and Zeronian, Hudson, and Peters (1964) for readers who want to explore the history of periodate oxidation of carbohydrates.

While the use of periodate oxidation for analytical purposes has diminished due to the development of other analytical tools for structural characterization, it is now applied in polysaccharide chemistry for materials engineering. The aqueous solvent conditions that are called for in periodate oxidation make it suitable for forest products and have the potential to comply with green chemistry guidelines (Anastas & Eghbali, 2010). As mentioned, the initial focus of periodate oxidation was on

* Corresponding author at: Department of Chemistry and Chemical Engineering, Chalmers University of Technology, Gothenburg, Sweden.
E-mail address: tiina.nypelo@chalmers.se (T. Nypelö).

https://doi.org/10.1016/j.carbpol.2020.117105
Received 30 June 2020; Received in revised form 11 September 2020; Accepted 12 September 2020
Available online 19 September 2020
0144-8617/© 2020 The Authors. Published by Elsevier Ltd. This is an open access article under the CC BY license (http://creativecommons.org/licenses/by/4.0/).

polysaccharide analysis, but analytical investigations (Bobbitt, 1956) had already highlighted its preparative use. The materials engineering view was also introduced early on (Zeronian et al., 1964).

The structures of interest in this review are forest resources, which include wood fibers, particles, and fibrils. Hemicelluloses are treated as well. Hemicellulose extracts are mostly monomeric, oligomeric, and polymeric. However, as they are often linked within the wood polysaccharide matrix, we think that their treatment in the context of modulation of hierarchies is deserved. Periodate oxidation leads to altered intra- and inter-fiber bonding and hence many properties such as strength, strain, and response to temperature are subsequently altered. We review these alterations with respect to the oxidized moieties that are produced. We also discuss the crystallinity of the oxidized products and their analysis. We focus on the literature published over the last 10 years (2010–2020) with some exceptions (mostly in the discussion about analytics). Regarding hemicellulose periodate oxidation, due to scarcity, we also address less recent literature.

The structures that are covered and their nomenclature are cellulose fibers (refers to pulp fibers), cellulose nanofibrils (CNF), cellulose nanocrystals (CNC), paper (made of pulp fibers), and films (made of CNF, CNC, or solutions). The oxidized products will be referred to as periodate-oxidized or dialdehyde and dicarboxyl or dialcohol cellulose/hemicellulose as applicable. The focus is on forest resources, but some literature on other materials (e.g., cotton) is included when it is applicable to forest resources.

The motivation of this review is to summarize the current status of utilizing periodate oxidation for materials engineering. The hypothesis is that periodate oxidation can generate a versatile portfolio of polysaccharide hierarchies on various levels. There are four sub-ambitions in this review: *Chapter 2* gathers key analytical procedures for degree of oxidation characterization; *Chapter 3* describes structural modulation during oxidation; *Chapter 4* summarizes selected properties of oxidized hierarchies; and *Chapter 5* discusses the current status and potential of industrial processing and reactant recycling.

2. Analysis of degree of oxidation

Periodate oxidation of cellulose leads to the introduction of two aldehyde groups on a carbohydrate monomer unit. The reactive aldehyde functionalities can be present as masked forms: hydrates, hemialdals, and hemiacetals (Fig. 1). More specifically, Spedding (1960) lists (1) free aldehyde, −CHO; (2) hydrated aldehyde, −CH(OH)2; (3) hemialdal, −CH(OH)−O−CH(OH)−; and (4) hemiacetal, −CH(OH)−O−CH2. Intra-chain and intra-anhydroglucose unit hemiacetal formation is possible between C2/C6 and C3/C6 and hemialdal C2/C3. Inter-chain hemiacetal formation takes place between C2/C6 and C3/C6 (Sulaeva et al., 2015).

Oxidation at positions C2 and C3 leads to the cleavage of the ring, which alters the structure of the polysaccharide chain. The literature on the fundamentals of the increase in backbone flexibility of the polymer is scarce. However, “hairy” or sterically stabilized CNCs where oxidation introduces flexible chains on the particles or the ends were reported. The flexible chains enable colloidal stability, which stems from the polymeric extensions (Chen & van de Ven, 2016; Leguy et al., 2018; Sheikhi & van de Ven, 2017; Van De Ven & Sheikhi, 2016; Yang & van de Ven, 2016).

Oxidation of polymeric xylan from wood with a high degree of oxidation (DO), 92 %, led to a complete transformation of the xylan structure and formation of poly(2,6-dihydroxy-3-methoxy-5-methyl-3,5-diyl-1,4-dioxane) (Amer et al., 2016). Painter and Larsen (1970) reported hemiacetal formation between oxidized and nonoxidized moieties. Börjesson, Larsson, Westman, and Ström (2018) reported alterations in oxidized arabinoxylan glass transition and took that as an indication of increased chain flexibility. They also reported a decrease in arabinose content, which indicates that the oxidation took place at the arabinose units rather than on the xylose. Fu et al. (2020) reached an 84 % DO of xylan, and Köhnke, Elder, Theliander, and Ragauskas (2014) reached an aldehyde content up to 6 mmol/g of xylan.

A selection of analytical methods quantifying the functional groups of the oxidation product is presented in Table 1. The direct observation and thus calculation of aldehyde groups in oxidized carbohydrates is a

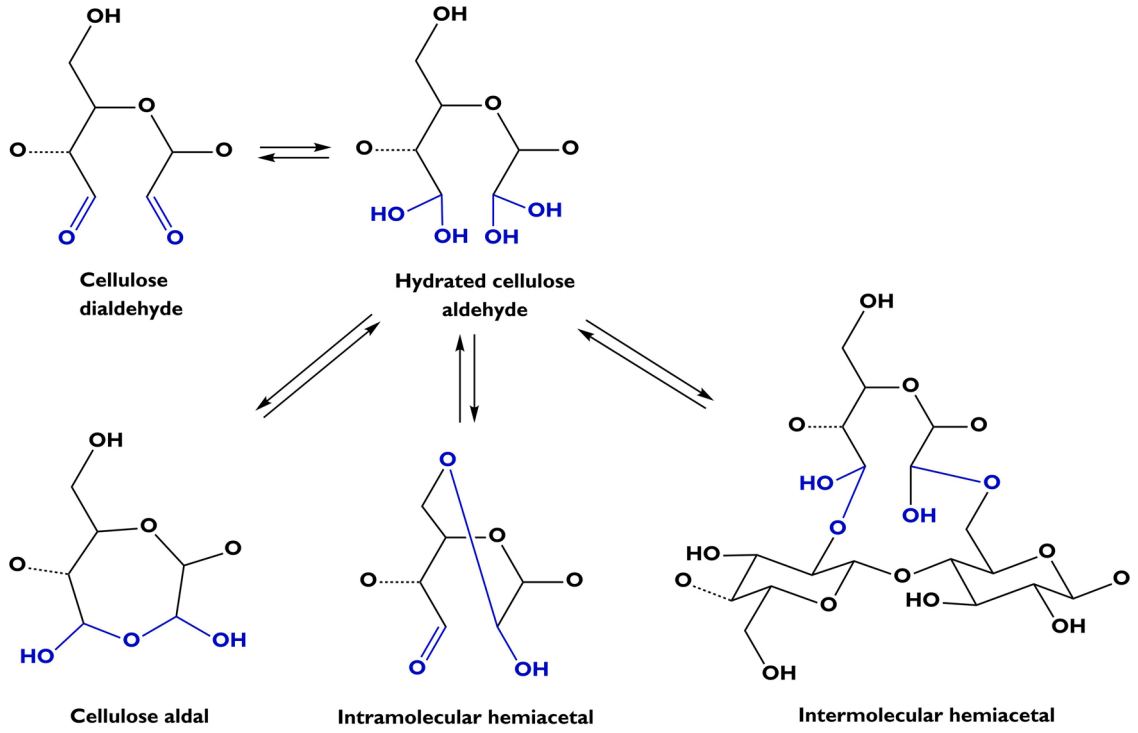

Fig. 1. Overview of linkages (inter- and intra-hemiacetals and hemialdals) in aqueous systems of dialdehyde cellulose. The figures have been drawn by the authors with ChemDraw.

Table 1
A selection of analysis methods for determination of degree of oxidation (DO) and functionality of periodate-oxidized polysaccharides.

Analysis class	Applicable to	Methods
Spectroscopy	Solutions, suspensions, films, solids	DO from detection of consumption of periodate based on UV-absorbance (290 nm); Detection of functional groups with NMR, FTIR absorbance at 1730−1740 cm^{-1}; Fluorescent labeling of aldehyde groups with 2,4-dinitrophenyl hydrazine and UV-absorbance analysis (Tummalapalli & Gupta, 2015)
Spectrometry	Solutions	Degree and pattern of oxidation via mass spectrometry (Lipniunas et al., 1992) and MALDI-TOF (Kochumalayil et al., 2013)
Chromatography	Solutions	Carbazole-9-carboxylic acid [2-(2-aminooxyethoxy)ethoxy]amide labeling combined with GPC analysis (Röhrling et al., 2002)
Titration	Solutions, suspensions	Iodometric titration of formic acid or periodate (Babor et al., 1973; Hay et al., 1965); Colorimetric determination of periodate (Avigad, 1969) Aldehydes converted to oximes with hydroxylamine hydrochloride. Titration of acid product with NaOH. Oxidation of the aldehydes to carboxyl groups and their subsequent conductometric titration (Liimatainen et al., 2012) Determination of consumption of hydroxyl ions per aldehyde group (Pommerening et al., 1992; Sun et al., 2015)
Elemental analysis	Solutions, suspensions, films, solids	Elemental composition of, for example, nitrogen in oxime modification (Vicini et al., 2004)
Carbohydrate composition	Solutions, suspensions, films, solids	HPLC analysis of carbohydrate composition before and after oxidation for estimation of DO (Börjesson et al., 2018)

cumbersome process due to masking of the aldehydes. Therefore, indirect methods are preferred. The determination of DO from consumption of periodate based on ultraviolet (UV)-absorbance at 290 nm during oxidation is often employed. The DO of the product of xylan has further been determined by analysis of the Fourier-transform infrared spectroscopy (FTIR) absorbance intensity of the band at 1730 cm^{-1} (Börjesson et al., 2018). Identifications of the aldehyde groups in the oxidized species utilizing infrared (IR) and nuclear magnetic resonance (NMR) analyses are numerous, but the findings are not always consistent. Some reasons behind this can be that a DO of 12 % is reported to be required to detect carbonyl and hemiacetals in oxidized cellulose (Kim, Kuga, Wada, Okano, & Kondo, 2000) and that it has been hypothesized that after oxidation the carbonyls form hemiacetals and cannot be detected as aldehydes (Guigo, Mazeau, Putaux, & Heux, 2014).

Spedding (1960) noted on the availability and state of functional groups in oxidized products, relying on FTIR spectroscopy. Free aldehyde groups were present in air-dried periodate-oxidized cellulose. Their number slightly increased upon drying over phosphoric anhydride at 30 °C and considerably when heated to 105 °C. The aldehyde groups that were liberated during heating were, originally, mostly bound in hemialdals, while the rest consisted of free aldehyde, hydrated aldehyde, and hemiacetal groups.

Kim et al. (2000) analyzed a dried oxidized cellulose product and assigned the band at 1740 cm^{-1} to the carbonyl group and the one at 880 cm^{-1} to hemiacetals and hydrated forms. Aldehyde analysis of cellulose based on the band at 1730 cm^{-1} was also reported (Tian & Jiang, 2018). In liquid state NMR, the lack of the carbonyl signal expected at 175−180 ppm was justified by the hydration of aldehydes or by the formation of hemiacetals with the remaining hydroxyl groups (Kim et al., 2000). Indeed, solid-state ^{13}C NMR spectroscopy data have shown that readily oxidized carbonyl groups are transformed into hemiacetals by recombining with vicinal hydroxyl groups (Azzam, Galliot, Putaux, Heux, & Jean, 2015).

Similarly, Sun, Hou, Liu, and Ni (2015) showed the appearance of the carbonyl band at 1735 cm^{-1} in an FTIR analysis of oxidized CNCs. They also reported a band at 885 cm^{-1} [as did others; see, e.g., Tian and Jiang (2018)], which they attributed to hemiacetal vibrations. They further concluded that a weakened OH absorbance at 3413 cm^{-1} and 1059 cm^{-1} as a result of oxidation indicates that aldehyde or hemiacetal groups were present. Kriechbaum and Bergström (2020) identified carbonyls at 1740 cm^{-1} and, due to the disappearance of the band, concluded that they were consumed by a follow up reaction. FTIR spectroscopy of carbonyl at 1732 cm^{-1} (Fu et al., 2020) and NMR spectroscopy (Köhnke et al., 2014) have been applied in hemicellulose analyses. Mass spectrometry has been used to determine oxidation locations and frequency (Kochumalayil, Zhou, Kasai, & Berglund, 2013; Lipniunas, Angel, Erlansson, Lindh, & Nilsson, 1992).

Labeling with UV-absorbing 2,4-dinitrophenyl hydrazine and detection of the unreacted molecules by UV-absorbance at 357 nm has been demonstrated for pectin and could be utilizable for cellulose and hemicelluloses (Tummalapalli & Gupta, 2015). Fluorescent labeling with carbazole-9-carboxylic acid [2-(2-aminooxyethoxy)ethoxy]amide combined with gel permeation chromatography (GPC) analysis has also been applied (Röhrling et al., 2002).

There are several titration methods for aldehyde quantification. They are based on titration of acid products during aldehyde derivatization or formation, residual periodate, or the aldehyde groups. Iodometric titration is a traditional method, and it is applicable to monosaccharides when detection is based on formic acid formed during oxidation (Babor, Kaláč, & Tihlaric, 1973). Iodometric titration can also be used to determine periodate (Hay, Lewis, & Smith, 1965) in the oxidation by titrating iodine ($I_2 + 2S_2O_3^{2-} \rightarrow 2I^- + S_4O_6^{2-}$). Periodate concentration can also be colorimetrically determined, as periodates rapidly oxidize the violet ferrous-2,4,6-tri-2-pyridyl-s-triazine complex to a colorless compound (Avigad, 1969). For polysaccharides, the formation of oxime by the reaction of aldehyde and hydroxylamine hydrochloride results in the release of one mol of hydrochloric acid for every mol of aldehyde. The released acid can be titrated with bases like sodium hydroxide. The amount of aldehyde is directly connected to the consumption of the base; that is, one mol of sodium hydroxide equals one mol of aldehyde. Titration of aldehyde with stoichiometric consumption of hydroxyl ions per aldehyde group is applied for direct aldehyde determination from the oxidation product (Pommerening, Rein, Bertram, & Muller, 1992; Sun et al., 2015). The aldehyde content can also be quantified by analyzing the carboxylic acid content (Liimatainen, Visanko, Sirviö, Hormi, & Niinimäki, 2012) of carboxylic acid derivatives of dialdehyde polysaccharide. Elemental analysis can be applied to determine, for example, the nitrogen content of the oxime-modified aldehydes (Vicini et al., 2004).

Aldehyde content is usually expressed as μmol/g (or mmol/g), describing the molar content of aldehydes per gram of the oxidized product. Another way to present the periodate-oxidized product is by describing the DO, which represents the number of oxidized anhydroglucose units in the polysaccharide. The DO is related to the aldehyde content, as two aldehyde groups are formed by the oxidation of one anhydroglucose unit. It should be noted that the degree of substitution, generally used in cellulose chemistry, is inconvenient in the context of periodate oxidation. The degree of substitution assumes that all the hydroxyl groups of cellulose are reactive, and thus the maximum degree is three, whereas in periodate oxidation, theoretically, only secondary hydroxyl groups react, leading to a maximum degree of substitution of two.

Carbohydrate content can be analyzed via acid hydrolysis and subsequent analysis of the monomers using, for example, high-performance liquid chromatography (HPLC) analysis. This method does not identify chemical functionality but relies on observing changes in carbohydrate composition. However, Abdel-Akher et al. (1952) and Hay et al. (1965) proposed carbohydrate composition analysis of periodate-oxidized moieties. In principle, the non-oxidized moieties are preserved and hence detected while the acyclic parts are cleaved. This technique has been utilized for polymeric carbohydrates (Börjesson et al., 2018). A comparison of the oxidation product to the carbohydrate composition after the oxidation can reveal the extent of the oxidation.

Consideration of the hierarchy of the structure becomes important in most of the analysis methods (Table 1). While identification of a modification within a fiber or fibril (vs. on the surface) is challenging with titration techniques, it is straightforward with elemental analysis. Spectroscopic evaluation (IR, NMR) of solids can be hindered by resolution (solid state vs. liquid state NMR) and the state of the functional groups, for example, as discussed above in the case of hydration of aldehydes and hemiacetal formation in a solution. Bobbitt (1956) acknowledged the challenge of purifying carbohydrate materials after oxidation. Indeed, analysis of nanomaterials with, for example, titration techniques can be challenging due to the fact that washing the nanosized product via filtration (unlike fibers) is often not possible, since solvents are retained in the material or cannot be separated from the material with a filtration that provides a convenient (short) dewatering time. Analysis of film material entails additional challenges. Ultrathin films on a support have restricted flexibility when it comes to NMR and UV–vis analyses, while X-ray reflectivity and IR analysis are applicable. The "ultrathin" refers to films with thicknesses of less than 100 nm (Kontturi & Spirk, 2019); hence they are limited by the penetration depth of the analysis and the amount of analyzable substance, which affects the signal-to-noise ratio during measurement and considerably increases measurement time. Measurement time is especially critical for X-ray--based techniques, because cellulose-based materials are prone to radiation damage, which can impact the results of the analysis. When it comes to self-standing films (typical thickness in the tens of micrometers), their analysis in solvents requires consideration of film intactness with respect to immersion/analysis time. In all film applications, the primary focus tends to be resolving spatial distribution. However, resolution at the molecular level is challenging. Visualization of oxidation locations has also been challenging due to the complex morphology of fiber materials and the overlap of spectroscopic bands of the various functionalities in the material. Recently, Imamura et al. (2020) analyzed chromatography paper that was oxidized in a periodate solution using micro-FTIR spectroscopy. They localized the carbonyl band at the fiber surfaces, but a homogeneity analysis remains a task for future research.

3. Structural modulation during oxidation

The starting materials for oxidation have predominantly been of high cellulose content (e.g., wood pulp), micro and nanocrystalline cellulose, and structures in between those. In Section 3.1, we introduce findings on the evolution of structures via oxidation. These phenomena involve breaking down larger matter into smaller entities, the formation of core-shell structures, fiber accessibility, and the oxidation mechanism. The analytical focus of this chapter is the development of crystallinity, which is discussed in Section 3.2.

3.1. Development of hierarchies via oxidation

Preservation or fractionation of fibrillar or particulate matter is of interest for materials engineering, as crystallinity can affect the thermal, mechanical, and permeation properties of materials. Periodate oxidation has been reported to decrease crystallinity but also to separate material into fractions of different sizes. The production of either CNFs or CNCs depends on the DO, mechanical disintegration, and chemical modification (Kekäläinen, Liimatainen, & Niinimäki, 2014; Sirviö, Visanko, Laitinen, Ämmälä, & Liimatainen, 2016; Sirviö, Honkaniemi, Visanko, & Liimatainen, 2015). The formation of different cellulosic nanospecies is related to the oxidation mechanism (Sirviö, Hasa et al., 2015). At a low oxidation degree (aldehyde group content below 2.20 mmol/g), random oxidation of cellulose fibers resulted in the formation of long nanofibers after the introduction of charged groups followed by mechanical disintegration. Increase in the DO leads to the cluster mechanism taking place where the region near already oxidized portions of cellulose is more easily oxidized than pristine parts of fibers (Kim et al., 2000) and results in degradation. Generation of rod-like or spherical cellulose particles has been reported depending on the oxidation condition severity (Huang et al., 2020).

Chen and van de Ven (2016) showed that partial oxidation of kraft softwood pulp generated three products: fibrous cellulose, sterically stabilized nanocrystalline cellulose, and dialdehyde cellulose (which was soluble in water when heated). As oxidation time increased, the fraction of fiber material decreased, and the nanocrystals and dissolvable fractions increased. Errokh, Magnin, Putaux, and Boufi (2018) reported a degradation of cellulose fibers as the DO increased, and their separation into nanosized particles was completed by reduction with borohydride, which turned suspensions translucent and resulted in decreased size of the particles detected by light scattering. The periodate-chlorite oxidation of CNFs followed by reaction with Girard's reagent T was also reported to result in several fractions of materials. These included sterically stabilized CNCs, solubilized dialdehyde modified cellulose, electrosterically stabilized CNCs, solubilized dicarboxylated cellulose, cationic CNCs, and solubilized quaternary amine-modified cellulose (Sheikhi & van de Ven, 2017). Oxidation without a loss of particulate matter in the water-soluble fraction is currently a challenge.

Liu et al. (2019) showed that alkaline periodate oxidation of cellulose leads to the formation of CNCs in various cellulose sources, including microcrystalline cellulose, fibers, and sawdust. The formation of CNCs was attributed to the formation of anionically charged dimeric orthoperiodate ions at pH 10 having a lower oxidation potential (Dryhurst, 2015) and thus leaving the crystalline region intact. Under alkaline conditions, oxidized cellulose domains are degraded due to beta-alkoxy fragmentation, resulting in the formation of CNCs. Similar methods were previously utilized in Pickering emulsion, identified as self-terminating isolation of CNCs (Liu et al., 2018).

The concept of an amorphous shell and a core of highly ordered CNFs has been proposed via periodate oxidation (Larsson, Berglund, & Wågberg, 2014a; Larsson, Berglund, & Wågberg, 2014b; Larsson & Wågberg, 2016). Larsson et al. (2014b) applied periodate oxidation to create core–shell modified CNFs where the cellulose core is surrounded by a shell of ductile dialcohol cellulose created by heterogeneous periodate oxidation followed by borohydride reduction of the native cellulose in the external parts of the individual fibrils.

Periodate oxidation has been reported on in the context of increased fiber accessibility. Hao, Wang, Zhao, Fang, and Cai (2018) modified cotton fabrics with periodate oxidation. They used a determination of the iodine sorption value to elucidate fiber accessibility. A higher iodine sorption value was reported for oxidized fibers compared to the starting material, indicating increased accessibility. This was taken as an indication of structural change and an increase in amorphous area. Shaikh, Adsul, Gokhale, and Varma (2011) reported that a DO above 50 % resulted in easier hydrolysis of the cellulose by cellulase. Oxidation of xylan with periodate and chlorite into dicarboxylates has also been used to enable enzymatic digestion (Matsumura, Nishioka, & Yoshikawa, 1991).

Liu et al. (2012) reported that the DO corresponded to a decrease in crystallinity. They summarized the involved reactions as the C2/C3 cleavage and conversion to dialdehyde cellulose, degradative beta-cleavage, and acid hydrolysis of the glycosidic bonds. Increasing periodate concentration between 0.3 and 0.9 mol/L led to a higher

reaction rate for aldehyde generation than cellulose degradation. Temperature plays a significant role, as it increases the aldehyde content at the expense of accelerated degradation. This has also been reported elsewhere (Sun et al., 2015). Oxidation reactions on cellulose can be quite sensitive to the allomorph used as the starting material. Siller et al. (2015) reported that periodate oxidation proceeded faster for cellulose II (regenerated cellulose) than cellulose I (native cellulose); however, they suggested that the major influencing factor was the overall crystallinity rather than the allomorph. Yuldoshov, Atakhanov, and Rashidova (2016) showed that the oxidation rate was dependent on the starting material, and nanocellulose oxidized faster than cotton or microcrystalline cellulose, which suggests that the hierarchical structure of the starting material as a whole has a significant effect on the process.

A periodate oxidation mechanism has been proposed where the oxidation attacks the cellulose substrate heterogeneously and produces hinges on the oxidized locations that are susceptible to peeling off (Kim et al., 2000). Furthermore, due to the local loss of crystalline order, oxidation leads to an increased susceptibility to peeling off of neighboring groups. In the model of Kim et al. (2000), a heterogeneous reaction leads to isolated oxidized domains along the microfibrils. Acid hydrolysis after oxidation leads to shorter cellulose fractions in the case of periodate-oxidized cellulose than directly hydrolyzed cellulose particles (Kim et al., 2000). These observations were taken as an indication that periodate oxidation proceeds by forming dialdehyde groups in longitudinally spaced, bandlike domains. Labeling of the features with gold particles led to light coverage, indicating non-uniform oxidation products (Kim et al., 2000). Calvini and Gorassini (2012) have proposed a non-random oxidation mechanism based on oxidation of the accessible core of fibers and a simultaneous oxidation of the fiber surface. However, it has also been reported that highly ordered regions in cellulose are even affected by oxidation at low degrees of oxidation (Potthast, Kostic, Schiehser, Kosma, & Rosenau, 2007; Potthast, Schiehser, Rosenau, & Kostic, 2009). In fact, the early studies of Goldfinger, Mark, and Siggia (1943) revealed two rate constants of oxidation of which the faster was determined to take place preferentially in the amorphous domains, and the second was determined to be related to the crystalline domains.

The recent findings of Koso et al. (2020) involved dissolution of periodate-oxidized cellulose in a basic electrolyte for 2D NMR analysis. The dissolution resulted in the liberation of fractions of oligomeric, dimeric, and monomeric species. In addition, polymeric cellulose chains that originated from the core of the CNCs were resolvable. These findings lend support to the oxidation mechanism that involves peeling off cellulose fractions from the oxidation surfaces.

Chen and van de Ven (2016) suggest that, initially, periodate reacts preferentially with the amorphous cellulose regions that are sandwiched between crystalline regions in CNFs. They also report that further oxidation of sterically stabilized CNCs that contain protruding dialdehyde modified cellulose chains leads to a gradual decrease in the lengths of the particles while retaining their widths. This is referred to as an indication that periodate oxidation creates a reaction front at the boundary of amorphous and crystalline regions that advances towards the crystalline regions (Chen & van de Ven, 2016).

Conley, Whitehead, and van de Ven (2016) showed that sequential oxidation with sodium meta-periodate and sodium chlorite that converts cellulose to dicarboxyl cellulose led to detachment of these chains from the CNCs surfaces and a consequent reduction in crystal width. Some chains remained only partially oxidized and did not detach but resulted in CNCs with attached dangling chain ends. Further oxidation also resulted in a reduction of crystal length. In the study of Leguy et al. (2018), the hydrodynamic diameter determined by dynamic light scattering of CNCs decreased as the DO increased, indicating a decrease in the dimensions of the crystals. Electron microscopy investigations revealed that a slight size reduction took place in length rather than in width. A size reduction of rice husk microcrystalline cellulose after oxidation has been reported as well (Madivoli, Kareru, Gachanja, Mugo, & Makhanu, 2019).

The various oxidation mechanisms are schematized in Fig. 2 according to our interpretation of the literary descriptions above. Oxidation proceeds either in the dislocations or crystalline domains of cellulose. The dislocations (Nishiyama et al., 2003) represent the areas that are often referred to as amorphous regions. Attack at both dislocations and crystalline domains can lead to separation of the higher hierarchies into lower ones. Attack on dislocations produces dangling chain ends that can lead to fractionation into smaller particles and further peeling off of molecule fractions. The same outcome can be achieved by attack on crystalline regions. The sizes of the particulate fractions should vary depending on the mechanism of the degradation and, as described above, the findings on this are divergent.

3.2. Determination and development of crystallinity

Analysis of cellulose crystallinity is an entire field of its own, where the challenges of crystallinity quantification arise from broad bands in crystallography and non-trivial baseline selection (French, 2020; Park, Baker, Himmel, Parilla, & Johnson, 2010). Periodate oxidization leads to a decrease in crystallinity as the DO is increased to such an extent that the challenges of broad bands and ambiguous baselines are amplified. We consider these challenges with respect to periodate-oxidized (originally) crystalline nanocellulose, but first we must describe the practice of cellulose crystallinity determination.

Several techniques have been used to determine the crystallinity of cellulose-based materials, such as solid-state NMR (Röder et al., 2006; Teeäär, Serimaa, & Paakkari, 1987), IR spectroscopy (Nelson & O'Connor, 1964a, 1964b; Široký, Blackburn, Bechtold, Taylor, & White, 2010), Raman spectroscopy (Röder et al., 2006), and X-ray diffraction (XRD) (Bayani, Taghiyari, & Papadopoulos, 2019; Park et al., 2010; Röder et al., 2006; Teeäär et al., 1987; Thygesen, Oddershede, Lilholt, Thomsen, & Ståhl, 2005). Typically, the methods that are sensitive to the local environments of nuclei (e.g., NMR spectroscopy) provide larger values of the fractional crystallinity than those sensitive to long-range order (X-ray diffraction). XRD is probably most frequently used, as this method was first applied to verify the structure of cellulose (Meyer & Misch, 1937). In most cases, a qualitative comparison is sufficient; e.g., a broadening or disappearing of peaks suggest a loss of crystallinity. Using only qualitative analysis, however, does not allow one to reliably compare data from different studies. Various methods have been used to quantify crystallinity, but the results tend to vary depending on the choice of measurement and analysis method (Ahvenainen, Kontro, & Svedström, 2016; French, 2020; Park et al., 2010; Terinte, Ibbett, & Schuster, 2011; Thygesen et al., 2005).

One of the most commonly used ways of calculating crystallinity is the peak height Segal method (Segal, Creely, Martin, & Conrad, 1959). X-ray apparent crystallinity (%) of cellulose is calculated from the height ratio between the intensity of the crystalline peak and the non-crystalline intensity, for which an intensity value is chosen manually. In the case of cellulose, the most commonly chosen crystalline peak is the 002 reflection, which is present between $22-24^\circ$ 2Θ, while for the non-crystalline value, typically the intensity at about 18° (the minimum between peaks) is chosen. This empirical method can provide only relative values, because the measured spectrum always contains contributions from amorphous regions in the position of the crystalline peaks as well. Moreover, overlapping of crystalline peaks has an additional influence on the results (French, 2020). Despite the simplicity and the popularity of this method, it is not so reliable, as it overestimates crystallinity. Another difficulty is that the measured peak-intensities are affected by the structure's preferred orientation; therefore, the measured intensity (peak height) ratio and apparent crystallinity can be strongly influenced by the orientation (Agarwal, Ralph, Reiner, Moore, & Baez, 2014). A 2D area detector or a rotating stage can be used to study or to circumvent the orientation effect.

Analysis of peak area instead of peak height can yield more reliable

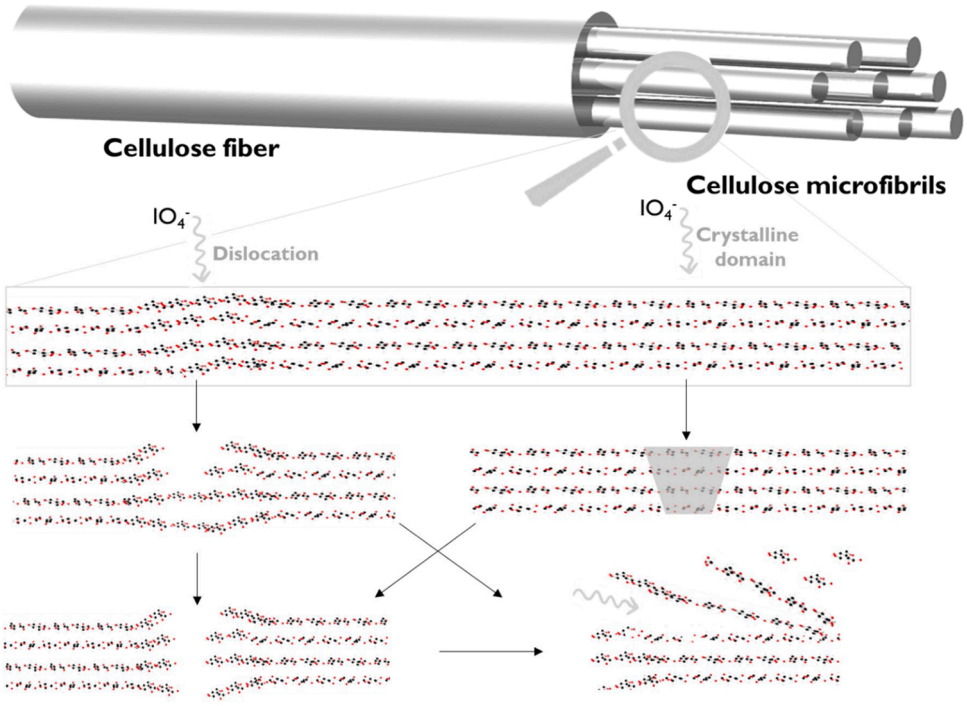

Fig. 2. Summary of commonly proposed mechanisms of structure development during periodate oxidation. The figures have been drawn by the authors with POV/Ray.

crystallinity values. One can either subtract the signal of an amorphous sample or deconvolute the measured peaks. The challenge when using the first option for wood-based materials, especially cellulose, is to find a non-crystalline representative. One solution could be to study a series with varying crystallinity from fully amorphous to perfectly crystalline, which could be used for calibration; however, this kind of approach is rarely available and would not solve the problem of comparability between studies. That leaves deconvolution, where the apparent crystallinity is comprised of areas under the crystalline peaks in the diffraction pattern corresponding to the Miller indices, and likewise, the intensity of the non-crystalline signal is the area under the non-crystalline peak of the cellulose diffraction pattern (Park et al., 2010).

For deconvolution, a decision on the background is essential to avoid uncorrected non-sample contributions (e.g., thermal diffuse scattering, Compton scattering, air scattering, diffraction of the sample holder, etc.), which could lead to reduced crystallinity values (Thygesen et al., 2005). Subtraction of the empty sample holder's signal is a straightforward though rarely applied method for removing the non-sample-based diffraction signal. The next step is to choose the number and shape of peaks to fit. The typical peak deconvolution method uses only visible peaks and thus is likely to attribute some of the crystalline intensity to amorphous components or the background (French, 2020). The Rietveld method (Rietveld, 1969) has a large number of variable parameters and a plethora of unique data points to guide the refinement. In most cases, during deconvolution, four (101, 10$\bar{1}$, 002, and 040) (He, Cui, & Wang, 2008) or five crystalline peaks (101, 10$\bar{1}$, 021, 002, and 040) (Garvey, Parker, & Simon, 2005; Hult, Iversen, & Sugiyama, 2003) are fitted using Gaussian (Hult et al., 2003; Teeäär et al., 1987), Lorentzian (He et al., 2008), and Voigt (Garvey et al., 2005; Rodrigues Filho et al., 2007) functions. By analyzing the results, one can potentially distinguish between the crystallinity of different polymorphs of cellulose as well (Xing, Gu, Zhang, Tu, & Hu, 2018). Recently, French (2020) highlighted some of the most common errors during the evaluation of crystallinity and showed how the latest methods are focused on signaling the importance of better treatment of the amorphous component and pointed out the significance of the chosen function type in crystallinity analysis.

Yao, Weng, and Catchmark (2020) studied three types of cellulose after extensive ball milling. Based on the XRD curves, they were highly amorphous, exhibiting nearly identical profiles. They suggested that short-range order within a glucose unit and between adjacent units survives ball milling and generates the characteristic amorphous XRD profiles. To describe the amorphous XRD profile, a Fourier series equation was used, which they found more suitable than the commonly used Gaussian shape. The sustained ball milling dismantled the crystalline structure, and the atomic spacings within the glucan chain, which persists through ball milling, provide the signal of the amorphous cellulose. This can be referred to as short-range order, which is smaller than the persistence length. Bates et al. (2006) have hypothesized that by using a random close packed (RCP) model, such amorphous regions retain inherent short-range order, which was recently demonstrated for thin films (Jones et al., 2020). As the methods improve, establishing whether all complete preparations of amorphous cellulose give the same diffraction pattern becomes feasible (French, 2020).

While cleavage of the glucopyranose ring and introduction of aldehyde groups at C2 and C3 is understood on the molecular level, the action on supramolecular cellulose structures is less clear. Periodate oxidation decreases cellulose crystallinity as the DO increases (Kim et al., 2000), which has been attributed to oxidation taking place in the crystal structure. It was further suggested that the loss in crystallinity results from the opening of the ring and consequent restructuring of the order. This has been further supported by observation that the cellulose crystals get smaller with oxidation (Sun et al., 2015). Guigo et al. (2014) have shown that low DO (carbonyl content 0.38–1.75 mmol/g) cellulose microfibrils had been oxidized exclusively at their surface. In this case, the cellulose did not seem to be much affected by the oxidation, and the crystallinity reduced only slightly at higher DO conditions. Xu and Huang (2011) reported a slight increase in crystallinity after mild periodate oxidation, possibly due to partial dissolution of the oxidized fraction. This could be attributed to the higher reactivity of amorphous cellulose. Kim et al. (2000) showed that the fibrillar structure of microcrystalline cellulose was retained in the oxidation (10.7 mol $NaIO_4$

for 1 mol of glucopyranose).

Liu et al. (2012) found three reactions that relate to the evolution of crystallinity in the periodate oxidation system. The fast initial attack of periodate happens in the amorphous region; the second is a slow reaction on the surface of crystallites, followed by the oxidation of the crystalline core. They also reported improved oxidation of the amorphous region of cellulose at high concentrations. These findings, in accordance with the mechanisms in Fig. 2, can explain how the range of changes in crystallinity depends on the parameters used during oxidation. If the amorphous regions react first, a mild oxidation will not significantly affect crystallinity. However, as soon as the crystalline core also takes part in the oxidation, the increasing DO results in decreasing crystallinity.

Crystallite width analysis (with an increasing DO) has shown that the periodate oxidation gradually works its way into the fibril and reduces crystallinity (Larsson et al., 2014a). In order to preserve the structural integrity of the fiber, the oxidation needs to be mild. Oxidation of CNCs was reported to require attention to the oxidant to cellulose ratio. A higher $NaIO_4$ to CNCs ratio up to 4 increases the aldehyde content, after which there is only a contribution to reduction in yield (Sun et al., 2015).

Fig. 3 presents a typical evolution of XRD response of periodate oxidation of CNCs -based material, revealing a strong decrease in crystallinity after 12 h, with a further decrease after 24 h when utilizing a CNC/$NaIO_4$ ratio of 1.5 and oxidation at room temperature. The crystallinity index was determined using the peak area method upon the deconvolution of the recorded curves by fitting Gaussian functions. Four peaks were fitted based on the available 2Θ regime; however, some peaks disappeared during the oxidation process. After 24 h, only the most intense 002 peak remained. The crystallite width was calculated using the full width at half maximum (FWHM) values of the 002 peak. The crystallite width (denoted in Ångströms in Fig. 3) did not decrease significantly after the milder oxidation but dropped notably during longer treatment.

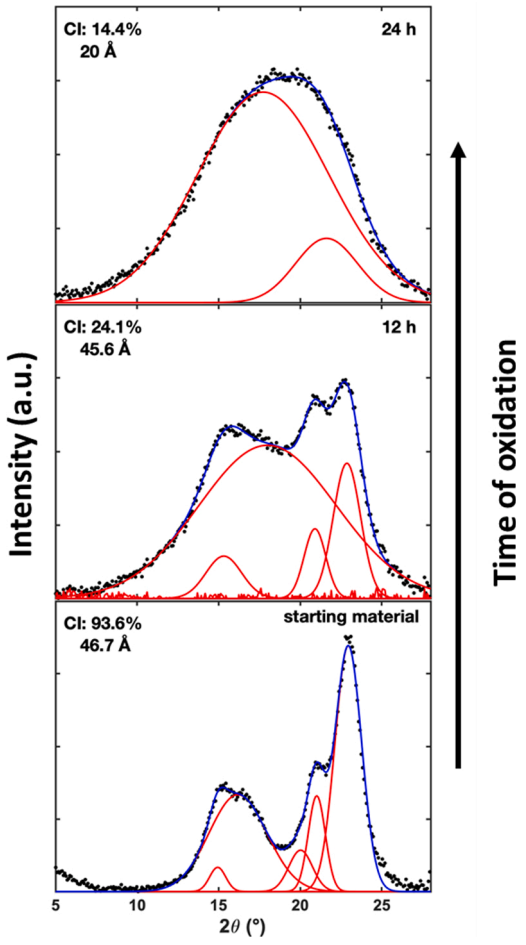

Fig. 3. Diffractogram showing deconvolution of cellulose nanocrystals: starting material and periodate-oxidized with oxidation times of 12 and 24 h. (Data courtesy of Nypelö and Berke).

4. Properties of oxidized hierarchies

4.1. Functionality and stability

The chemical functionality that can be generated via periodate oxidation includes aldehydes, carboxyls, alcohols, and any follow-up chemistry stemming from them, such as sulfonation (Hou, Liu, Liu, & Bai, 2007; Rajalaxmi, Jiang, Leslie, & Ragauskas, 2010; Sun, Liu, Dong, & Deng, 2017), cationization (Kim & Choi, 2014; Sirviö, Visanko, Laitinen et al., 2016; Yang & van de Ven, 2016), silanization (Lucia, Bacher, van Herwijnen, & Rosenau, 2020), and modification with boronic acid (Sajid et al., 2020). The selectivity of the oxidation to the C2/C3 leaves the C6 available to other modification and, for example, manufacturing of molecules with acetylation/phosphate in the C6 and sulfonation, amination, etc., from the aldehyde activation (Keshk, Bondock, El-Zahhar, & Haija, 2019; Rostami, Mathew, & Edlund, 2019) is reported. The functionalization of cellulose via periodate oxidation in combination with a modification such as carboxymethylation has been found to alter the physico-chemical properties by, for example, providing polyionic functionality (Chinga-Carrasco & Syverud, 2014) and viscosity, which entails applicability in, for example, 3D printing (Rees et al., 2015).

A combined periodate and chlorite oxidation can be used to introduce surface charges as carboxylate moieties (Kekäläinen et al., 2014; Liimatainen et al., 2012; Plappert, Liebner, Konnerth, & Nedelec, 2019). The introduction of charge aids controlled assembly of materials, since it enhances colloidal stability and hence improves material homogeneity (Plappert et al., 2019). Combining TEMPO/NaBr/NaClO with sodium periodate has been used to produce fully-oxidized 2,3,6-tricarboxycellulose from never-dried, bleached eucalyptus kraft pulp (Mendoza, Browne, Raghuwanshi, Simon, & Garnier, 2019), which resulted in water-soluble and water-insoluble fractions. Moreover, 2,3,6-tricarboxy cellulose also been produced via a combination of a nitroxyl-mediated reaction and periodate oxidation in a one-shot reaction from microcrystalline cellulose, yielding solubilized products (Coseri et al., 2015).

As discussed, the hydrated and connected states of aldehyde groups exist in solutions (Hurd, 1966). Due to the reactivity of oxidized functions, especially aldehydes, stabilization is often needed to control either chemical functionality or physico-chemical stability. Stabilization of aldehyde groups can be done by oxidation to dicarboxyl or reduction to a dialcohol product. Sodium borohydride can be applied to reduce the dialdehyde to dialcohol cellulose (Durán, Larsson, & Wågberg, 2016; Kasai, Morooka, & Ek, 2014; Larsson & Wågberg, 2016; Zeronian et al., 1964). Reduction with sodium borohydrate can lead to improved colloidal stability via the introduction of flexible chains on nanocrystal surfaces that provide steric stabilization (Leguy et al., 2018). Stability in films is a less explored territory. A study on the stabilization of oxidized crystalline cellulose films by further oxidation with ozone in dry form resulted in the conversion of the aldehyde groups to carboxylates (Nypelö, Amer, Konnerth, Potthast, & Rosenau, 2018).

The stability of the hemialdal/acetal structures is less defined in the literature. The level of moisture is important due to the reversibility of the hydrated state, the aldehyde state, and hemialdal/acetal formation (Erlandsson et al., 2018; Plappert et al., 2018). Dehydration is said to favor the formation of intra- and inter-molecular hemiacetal and hemialdal moieties. Toughness and elongation at break are increased by dehydration (Plappert et al., 2018). Narrowing down the bonding mechanism at a particular state of a wood polymer material is also

challenging due to the presence of residual moisture in (most) ambient conditions.

Reports on the properties of oxidized hemicelluloses are less extensive. Periodate oxidation of xylans has been reported to lead to water solubility (Amer et al., 2016; Fu et al., 2020). This is an asset in engineering applications, as wood-based hemicelluloses often have limited solubility in water.

Changes in molecular weight or functional group content with respect to storage time or time in solution are essential for oxidized product stability. Indeed, molecular weight can be indicative of more than the molecular weight of the starting or final polysaccharide product. We have identified three routes to molecular weight fluctuation in periodate-oxidized wood polysaccharides. Oxidation can lead to depolymerization, which decreases molecular weight. Hemiacetal formation with neighboring chains can lead to an increase in molecular weight. Molecular weight fluctuations can also occur as a combination of these two events.

Diverse outcomes are reported regarding degradation after solubilization. Some report severe degradation of cellulose shortly after solubilization (Sirviö, Visanko, Laitinen et al., 2016; Sulaeva et al., 2015) and further decrease of molecular weight when stored in a solution (Kim, Wada, & Kuga, 2004). The average molecular weight of cellulose was reported to decrease as the DO increased (Larsson et al., 2014a). Münster et al. (2017) observed aging of periodate-oxidized cellulose in solution and over the span of 28 days. Solubility and thermal stability were intact, and only a small decrease in aldehyde content was recorded. However, molecular weight increased during the observation period and was taken as an indication of hemiacetal formation. The molecular weight distribution was broadened due to the combination of depolymerization and crosslinking. To stabilize the solutions, a low pH value was deemed crucial, as it suppresses degradation processes by slowing down beta-elimination reactions, which lead to depolymerization. The study was performed on solubilized dialdehyde cellulose. Yan et al. (2018) found that the molecular weight decreased over time, independent of the DO, reaching a stable level after three months. The aldehyde content was noted to decrease over time as well (Yan et al., 2018). Sirviö, Liimatainen, Visanko, and Niinimäki (2014) showed that the reactivity of dialdehyde cellulose decreased during storage, and the carboxylic acid content of chlorite-oxidized dialdehyde cellulose stored for two weeks (at 4 °C in 25 % dry matter content) was only 68 % of the initial content.

In the case of arabinoxylans (not wood-based), the molecular weight decreased as the DO increased (Börjesson et al., 2018). Amer et al. (2016) showed that the molecular weight further decreased when the oxidized (wood-based) xylan was stored in a solution. Chemin et al. (2016) reported that depolymerization during oxidation of xylan depended on the oxidant:xylose ratio, where within 0.05, 0.20, and 1.00 depolymerization was noticed at 0.20 and above.

4.2. Inter- and intra-fiber, fibril, and crystal crosslinking

The aldehyde functionality on fiber and fibril surfaces has been used extensively for improving the strength of subsequent materials via inter- and intra-fiber crosslinking. The strength of paper products (Sun et al., 2015), wood fibers (Hou et al., 2007), and aerogels (Cervin, Johansson, Larsson, & Wågberg, 2016) was improved via the hemiacetal linkages at the inter-fiber bonds. Crosslinking of oxidized nanosized fibrils has been reported to lead to improved dry and wet stability due to the formation of intra- and inter-fibrillar covalent bonds and also noted to contribute to decrease in permeability of gas barriers (Henschen, Larsson, Illergård, Ek, & Wågberg, 2017; Larsson, Pettersson, & Wågberg, 2014; Larsson, Kochumalayil, & Wågberg, 2013). Durán et al. (2016, 2018) have reported increased material ductility as a result of periodate oxidation and subsequent reduction with borohydride. The combination of TEMPO and periodate oxidation has also been used to improve wet strength and stability of CNF membranes (Dahlström et al., 2020). Gorur, Larsson, and Wågberg (2020) utilized sequential TEMPO and periodate oxidation reactions to prepare self-fibrillating fibers from wood, where the fibrils could be liberated by external stimuli. Maintaining low pH values during sheet formation enabled intact fibers to form the paper supported by the hemiacetal linkages. The increase in pH value could then cause swelling and hydrolysis of the hemiacetal linkages and lead to fibrillation.

The formation of hemiacetals between aldehyde-containing cellulose fibrils has been elucidated by Erlandsson et al. (2018) in terms of the quantification of adhesion between the substrates. They identified 0.6 mmol/g as the lower limit for aldehyde content to enable crosslinked structures. Hemiacetal formation was shown to take place at pH 6.5, indicated by higher adhesion than at pH 12, where adhesion was reduced. The introduction of ethanol caused the re-established structure to disintegrate, and the hemiacetals could not reform. Hemiacetal formation in aqueous conditions was hence shown to increase the affinity between two oxidized substrates. Introducing the ethanol treatment while the chains were in contact could be used to strengthen a CNF aerogel structure by freezing followed by thawing and solvent exchanged in acetone (Erlandsson et al., 2018).

Aldehyde groups have been utilized to crosslink CNCs with polyvinyl alcohol matrices to improve mechanical properties. Polyvinyl alcohol fibers were reinforced via the introduction of dialdehyde cellulose, which produced a crosslinked structure (Hell, Ohkawa, Amer, Potthast, & Rosenau, 2018). In addition, the reactive aldehyde functionalities were present in the spun web. Sirviö, Hasa et al. (2015) have also reported acetal bond formation with polyvinyl alcohol and partially oxidized CNCs (aldehyde content of 2.20 and 3.86 mmol/g) that was followed by mechanical disintegration. Reduction of the aldehyde groups resulted in a poorer reinforcement effect of CNCs, indicating that acetal crosslinking indeed helps to improve the mechanical properties of polyvinyl alcohol. Similarly, the remaining aldehyde groups help to produce strong UV-absorbing polyvinyl alcohol films after imination of dialdehyde cellulose with *p*-aminobenzoic acid (Sirviö, Visanko, Heiskanen, & Liimatainen, 2016).

Reports of utilizing xylan in crosslinking reactions are less explored. Köhnke et al. (2014) oxidized xylan with periodate and combined it with hydroxyl-containing CNCs via hemiacetal bonds. This produced water-stable porous foams.

Periodate oxidation has been applied to alter cellulose materials' mechanical properties. The expectation is that the crosslinking with the hemiacetal formation increases strength. Indeed, oxidized CNC, used as a paper-strength additive, increased the dry tensile index by 32.6 % compared to the control sample (Sun et al., 2015). An increase in tensile strength from 15 to 23 MPa with the oxidation of paper fibers (Durán, Larsson, & Wågberg, 2018), as well as an increase in tensile strength as the DO increased (Durán et al., 2016), has been reported. However, a reduction in tensile strength has also been reported when cellulose membranes had been periodate-oxidized (Zhang, Kai et al., 2019). It may be that material strain is reduced if the material deformation is restricted, as can be the case when fibrils or fibers crosslink. Strain is important for ductility during hydrothermal forming. Indeed, the strength of a network of fibers with dialdehyde functionality yielded lower strain than a dialcohol form (Durán et al., 2018). Wet strength is mainly improved by periodate oxidation but not in the case of dialcohol cellulose (Durán et al., 2018; Larsson et al., 2014a). The mechanical properties of some materials reported in the literature have been compiled in Table 2. When the publication reports a series, the specimen with what appears to be the best performance is selected. The maximum strength at break of nanocelluloses is higher than that of fibers (Table 2). Strain at break and Young's modulus are diverse and do not allow generalization.

4.3. Thermal processing enabled by periodate oxidation

Periodate oxidation alters the thermal response of cellulose. Thermoplasticity of periodate-oxidized papers and films was monitored by

Table 2
Mechanical properties of cellulose fiber, fibril, and crystal materials prepared with or via periodate oxidation.

Material class	Material description	Tensile strength, dry/wet (MPa)	Strain at break, dry/wet (%)	Young's modulus, dry/wet (GPa)
Fibers (handsheets or paper)	Dialcohol DO 27 % bleached softwood kraft pulp (Larsson et al., 2014a)	93/-	11/-	5.9/-
	Dialdehyde DO 11 % bleached softwood kraft (Durán et al., 2018)	23/8	2/-	2.2/-
	Dialcohol DO 11 % bleached softwood kraft (Durán et al., 2018)	36/weak	4/-	3.5/-
Fibrils (as films)	DO 30 % (Hollertz, Durán, Larsson, & Wågberg, 2017)	192/-	3/-	8.7/-
	DO 6 % (Kriechbaum & Bergström, 2020)	115/10	10/17	3.9 GPa / 138 MPa
	DO 27 % (Larsson et al., 2013)	148/-	2/-	11.1/-
Cellulose nanocrystals (CNC)	Films of periodate-oxidized CNCs DO 81 % (Nypelö et al., 2018)	67/-		11.5/-
	Films of CNCs with 7.2 mmol/g aldehyde content. (Yang, Tejado, Alam, Antal, & van de Ven, 2012)	126/-		4.0/-
	Solubilized dialdehyde cellulose reinforced with 5 wt% CNCs (Plappert et al., 2018)	81−122/-		3.4–4.0/-
Regenerated cellulose	Regenerated cellulose membrane DO 12−353 μmol/g (Zhang, Kai et al., 2019)	113/-	8/-	

observing the storage modulus with respect to temperature, and transitions at 70−120 °C and 160−180 °C were assigned to the glass transition of dialcohol cellulose and to its flow state (Larsson & Wågberg, 2016; Morooka, Norimoto, & Yamada, 1989). Visualization of reference fibers and fibers modified to the degree of 40 % revealed a remarkable difference in appearance after hot-pressing with diminished fiber features and increased merge in the structure. Material softening was furthermore reported to be dependent not only on temperature but also on moisture content (Linvill, Larsson, & Östlund, 2017; Salmén & Larsson, 2018).

Codou, Guigo, Heux, and Sbirrazzuoli (2015) presented periodate oxidation of microcrystalline cellulose, revealing that thermal degradation shifted towards a lower temperature than pristine microcrystalline cellulose. The shift was emphasized with an increasing DO: the degradation temperature of 270 °C was reported for the pristine microcrystalline cellulose and a DO of 20 %, while it was decreased to around 160 °C for a DO of 85 %. The oxidized microcrystalline could be heated to 100 °C in compression and maintained that temperature for 2 h, resulting in drying and crosslinking. In the case of hemicelluloses, Kochumalayil et al. (2013) demonstrated periodate oxidation of xyloglucan and reduced the glass transition temperature by more than 100 °C.

Strong, Kirschbaum, Martinez, and Martinez (2018) utilized the structural changes of periodate oxidation to miniaturize chromatography paper via immersion into $NaIO_4$ followed by rinsing in water and drying, which led to shrinking of the paper. The phenomenon was not due to a thermal effect; however, the surface area reduction, denoted as the shrinking, was paired with a cross-sectional width increase and was associated with the behavior of thermoplastics. Hemiacetal formation was taken to be the reason for this behavior; the shrinkage was taken to be due to the fact that an intramolecular reaction cannot occur in a chair conformation, which leads to non-linear conformations and buckling. They further utilized the material for fabricating paper-based microfluidic devices (Strong, Schultz, Martinez, & Martinez, 2019). The shrinkage has also been observed and utilized in preparation of paper sensor chips with immobilized proteins (Imamura et al., 2020).

4.4. Covalent interactions with amine species

The functionalization of cellulose with aldehyde groups introduces the possibility of interactions with amine compounds via the Maillard reaction, Schiff base interactions, and imine formation. Kim and Kuga (2000) investigated the interactions between periodate-oxidized cellulose microbeads and aromatic amines. The oxidized cellulose was used as a stationary phase to separate various amine compounds. The interaction was identified as imine formation, which is an equilibrium reaction that requires the presence of unprotonated amine. The pKa value of the compounds is crucial for producing favorable conditions for the interaction. Kim and Kuga (2000) classified the compounds as functional groups with pKa values above 6 and 4–5.3. The separation was performed in pH 4–5.5. The imine reaction also involves the elimination of water that is catalyzed by acid, hence a pH value of 4–5 was chosen. The higher pKa-value compounds did not interact with the dialdehyde stationary phase. In the case of compounds with a pKa value in the range of the eluent pH value, there was affinity, which was more pronounced with higher aldehyde contents.

Kriechbaum and Bergström (2020) utilized the Maillard-type reaction at pH 6.5 to graft gelatin on periodate-oxidized CNFs. Dash, Foston, and Ragauskas (2013) and Kwak, Lee, Park, Lee, and Jin (2020) also combined gelatin to periodate-oxidized CNCs, and the latter showed that the crosslinking density increased as the level of oxidation of the CNCs increased. The amine groups of lysine were identified as the linking site and the crosslinking resulted in an increase in the modulus and thermal stability of the gelatin gels. A Schiff base reaction of periodate-oxidized xylan and gelatin has been employed for preparing crosslinked hydrogels (Fu et al., 2020). Taking a step back from gelatin, the denaturation temperature of collagen was increased via modification of dialdehyde CNCs (Pietrucha & Safandowska, 2015). An increase in dynamic moduli indicated the formation of covalent bonds during the crosslinking reaction. The formation of covalent bonds has also been used to link the oxidized cellulose to keratin (Song, Xu, Xie, & Yang, 2017).

The amine-containing polysaccharide chitosan has been used together with oxidized cellulose in various material endeavors. Oxidized cellulose sulfate was reacted with carboxymethyl chitosan (Stratz et al., 2019). A decreasing degree of sulfation at position C2/C3 led to increased aldehyde content, which in turn resulted in a shorter gelation time of the system. Oxidized nanocellulose was reacted with chitosan and transformed into crosslinked dialdehyde cellulose beads (Ruan, Strømme, & Lindh, 2018). A similar approach to crosslinking chitosan and dialdehyde cellulose has been applied to prepare films (Tian & Jiang, 2018), membranes with antimicrobial function (Bansal, Chauhan, Kaushik, & Sharma, 2016), and aerogels for oil absorption (Li, Shao et al., 2018). The chitosan interaction has also been used to crosslink periodate-oxidized cellulose with chitosan and to directly extrude it into fibers (Alam & Christopher, 2017). Dialdehyde cellulose-chitosan hydrogels have been used for the delivery of theophylline (Xu, Ji et al., 2019).

Amines can be introduced to cellulose fibers by combining periodate oxidation and reductive amination. The use of primary amines with different chain lengths to adjust the hydrophobicity (or amphiphilicity) of CNCs produced from aminated cellulose (Sirviö, Visanko, Laitinen et al., 2016). Due to the presence of both amine and alkyl functionality, the aminated CNCs showed good efficiency in mineral flotation (Laitinen et al., 2014, 2016). The amphiphilic properties of the aminated CNCs enabled their use as stabilizers in water-oil emulsion. Furthermore, bifunctional CNCs with carboxylic acid and amine moieties could be produced with sequential chlorite oxidation and reductive amination of periodate-oxidized cellulose (Ojala, Sirviö, & Liimatainen, 2016;

Ojala, Sirviö, & Liimatainen, 2018). The bifunctional CNCs showed good emulsion stabilization and thus could potentially be utilized in oil spill response, for example. Reductive amination has been employed to graft ethylenediamine to sulfuric acid hydrolyzed CNCs via activation with periodate oxidation (Jin, Li, Xu, & Sun, 2015). Reductive amination combined with periodate oxidation has also been introduced to prepare cellulose beads (Lindh, Carlsson, Strømme, & Mihranyan, 2014; Lindh, Ruan, Strømme, & Mihranyan, 2016).

A combination of polyethylene imine and benzyl modification of CNCs was used to generate particles for Pickering-type stabilization (Li, Ju, & Zhang, 2020). The hydrophilic amino and hydrophobic benzyl groups enabled pH-dependent emulsification or separation into oil and water phases. Decoration with benzyl groups has also been reported for a 15 % DO xylan via reductive amination (Chemin et al., 2015). Modification of periodate-oxidized cellulose with polyethyleneimine has been used to generate *N*-halamine functionalized cellulose membranes featuring antibacterial functionality (Zhang, Kai et al., 2019). Periodate-based glycine grafting and further complexation with Cu(II) also exhibited antibacterial activity (Xu, Shi, Lei, & Dai, 2020), as did zinc linked via a 4-aminobenzoic acid ligand (Noorian, Hemmatinejad, & Navarro, 2019) and a dialdehyde cellulose-silver composite (Li, Kang et al., 2018). The immobilized molybdenum complex has been established for catalysis (Sedri, Naeimi, & Mohammadi, 2018). Attaching Fe_3O_4 nanoparticles to dialdehyde cellulose particles has been proposed for protein concentration (Zhang et al., 2020).

Hao et al. (2018) reported that cellulase bound to oxidized cotton fibers more effectively than to non-modified fibers and accounted for this in terms of Schiff base formation. Tracing of the fluorescent-labeled cellulose revealed that the binding resided on the fiber surfaces. The large size of the cellulase protein was deemed to prevent access to the interior aldehyde groups and to remain on the fiber surfaces. Isobe et al. (2011) utilized activation via periodate oxidation to link proteins to cellulose also via the Schiff base reaction. Urease was linked to cellulose beads that were crosslinked with citric acid and activated by periodate oxidation (Lv, Ma, Anderson, & Chang, 2018). Soy protein isolate was reacted with oxidized microcrystalline cellulose (Salama, Shukry, El-Gendy, & El-Sakhawy, 2017). Activation of cellulose beads with periodate oxidation for protein attachment and immobilization of antibodies for selective capture of compounds from blood has been presented (Ettenauer et al., 2011). A similar approach was used to convert paper into a chemiluminescence immunoassay (Wang et al., 2012). Periodate-oxidized cotton yarn was used for trypsin enzyme immobilization with anti-inflammatory properties (Nikolic et al., 2010).

An adsorbent for heavy metals was prepared using dialdehyde cellulose grafted with graphene oxide, using triethylenetetramine as a crosslinking reagent (Yao, Wang, Liu, Yang, & Chen, 2019). A hydrazine-imidazoline modification has been suggested for precious metal separation from matrices (Hashem, Elnagar, Kenawy, & Ismail, 2020). Preparation of cysteamine-modified CNCs have been demonstrated for mercury removal (Li, Ju, & Zhang, 2019) and cysteine modification for arsenic (Chen et al., 2019). Periodate-oxidized cellulose strips have also been used for immobilization of glucose oxidase and horseradish peroxidase (Luo, Xia, Jiang, Yang, & Liu, 2019).

Adsorption of dyes such as Congo red has been demonstrated with epichlorohydrin-crosslinked cellulose that were further periodate-oxidized and Schiff base formation with the dye (Kumari, Mankotia, & Chauhan, 2016). At a pH value of 4, the maximum amount of Congo red was attached to the cellulose. Congo red adsorption has also been reported with chitosan crosslinked cellulose beads (Ruan et al., 2018) and films (Zheng et al., 2018). The amine-aldehyde interaction has also been studied for the oxidized hemicelluloses. Sodium periodate oxidation of xylan isolated from *Palmaria decipiens* yielded 2,3-dialdehyde xylan, which could then be reacted with *p*-chloroaniline (Barroso, Costamagna, Matsuhiro, & Villagran, 1997).

In addition to using the amine interaction for functionalization, they have been used for crosslinking. Preparation of pH-responsive hydrogels has been accomplished using diamines (Liu, Mai, & Zhang, 2017) and of solvent-responsive hydrogels by reaction with aniline (Zhang, Liu, Peng, Chen, & Zhang, 2019). Acyl hydrazones were employed as crosslinkers for dialdehyde cellulose (Xiao, Wang, Zhang, Chen, & Fu, 2019). The cleavage of the Schiff base bonds has been proposed for controlled drug delivery (Peng et al., 2019).

4.5. Other reactions

Periodate-oxidized cellulose structures have been shown to exhibit antimicrobial/bacterial activity against *Staphylococcus aureus, Methicillin-resistant Staphylococcus aureus,* Bacillus subtilis, Escherichia coli, *and* Salmonella typhimurium (Ge, Zhang, Xu, Cao, & Kang, 2016; Mou, Li, Wang, Cha, & Jiang, 2017; Zhang, Ge, Xu, Cao, & Dai, 2017). Periodate-oxidized cellulose has also been modified into 4-Amino-1,2,4-triazole-treated cellulose fabrics for antibacterial properties and metal sorption (Mohamed, Hassabo, Shaarawy, & Hebeish, 2017). Periodate-oxidized CNCs have been used to reduce silver ions and to stabilize the resulting silver nanoparticles (Xu, Jin, Wang, Chen, & Qin, 2019). This material, together with pulp fibers, was transformed into handsheets with antibacterial properties.

Covalent bonding of periodate-oxidized pulp with tannin was realized via a condensation reaction between a tannin molecule and aldehyde groups on the pulp (Ji, Xu, Jin, & Fu, 2020). Periodate-oxidized CNCs have been shown to be effective in the stabilization of emulsions with an acrylate monomer phase and intended for butyl methacrylate polymerization (Errezma, Mabrouk, Magnin, Dufresne, & Boufi, 2018). The stabilization was attributed to the reaction of bisulfite with aldehyde groups, forming an adduct that contributed to the initiation of the polymerization and nucleation of polymer particles. Oxidized hemicelluloses have been prepared for dispersant purposes (Konduri, 2017). Dialdehyde cellulose aqueous solutions have been used as adhesives for solid wood (Zhang, Liu, Musa, Mai, & Zhang, 2019).

5. Future of periodate oxidation – status of reagent recycling

Periodate is an environmentally hazardous chemical with a high acute toxicity; the lethal dose 50 % (LD_{50}) for sodium periodate is 58 mg/kg (mouse, intraperitoneal) (PubChem: sodium periodate, 2020), and the LD_{50} of reduced periodate (i.e., iodate) is 119 mg/kg (PubChem: Sodium iodate, 2020). Periodate is an expensive chemical, and since there is currently lack of the catalytic methods for periodate oxidation, the stoichiometric amount of periodate is consumed. The high cost of periodate can lead to the chemical costs (for a DO of 10 %) as high as 16, 500 €/ton (Liimatainen, Sirviö, Pajari, Hormi, & Niinimäki, 2013). Therefore, for ecological and economic feasibility, the recycling of periodate is of utmost importance.

On the industrial scale, periodate is produced by electrochemical oxidation of iodate (Brauer, 2012), and the electrochemical regeneration of spent periodate has been investigated (Janssen & Blijlevens, 2003), especially in the production of dialdehyde starch (Pfeifer et al., 1960). High operation costs and electrode sensitivity hinder the usability of electrochemical oxidation in periodate regeneration. Electrode sensitivity may be related to the partial dissolution and degradation of cellulose (and other polysaccharides) during periodate oxidation, resulting in complications during periodate regeneration. It has been shown that under mild oxidation conditions (aldehyde content around 0.4 mmol/g), 100 % of the spent periodate could be regenerated by using a minor excess (1.2–1.4 times) of sodium hypochlorite (Liimatainen et al., 2013). The regenerated periodate possessed a similar oxidation capacity to a first cycle compound. However, when the oxidation time was increased (and thus, the aldehyde content), regeneration efficiency notably decreased. The decrease in regeneration efficiency was assumed to be due to the formation of a small, dissolved cellulose degradation fraction, which could not be removed by ultrafiltration (20 kDa cut-off size). Nevertheless, with a moderate DO, the hypochlorite

was found to be a suitable chemical for periodate regeneration and could decrease the cost of the oxidation step from 16,500 €/ton to around 450 €/ton.

Although hypochlorite is an efficient and widely used commodity, it is a hazardous halogen-containing chemical. To decrease the use of halogen-based oxidants, other means of periodate regeneration have been investigated, including the use of peroxosulfate (Besemer, 2003) and ozone (Kesselmans & Peter, 1996). Ozone is a highly reactive oxygen species with a high oxidation power and is used, for example, in cellulose pulp bleaching. The regeneration of periodate with ozone has been shown to be pH-dependent. At acidic and neutral pH values, regeneration of periodate from iodate was not observed, whereas increasing the pH value to 13 resulted in complete regeneration conversion (Koprivica et al., 2016). The regeneration efficiency in a cyclic process of spent periodate after cellulose oxidation was found to be around 90 % due to the loss of a small portion of iodate during the workup procedure (i.e., iodate remained in the wet product). Nevertheless, at high pH values (14), the periodate precipitated, requiring the consumption of large quantities of acid for re-dissolution. Therefore, careful control of the pH value during the ozone-based recycling process is recommended.

Compared to hypochlorite recycling, regeneration of spent periodate with ozone is a fast reaction and can be performed under mild conditions. After mild oxidation of cellulose (2 % DO), spent periodate was regenerated after 20 min at room temperature (Koprivica et al., 2016). However, there is currently no information available on how dissolved cellulose components affect ozone regeneration, and further studies with highly oxidized cellulose should be conducted.

As mentioned before, the regeneration of spent periodate with hypochlorite and ozone works under alkaline conditions. However, periodate oxidation typically operates under neutral or acidic conditions, thereby requiring a pH adjustment. A pH adjustment increases operation costs and generates salts in the periodate solution. Although it has been shown that the presence of salts (e.g., sodium or lithium chlorides) could aid the periodate oxidation of cellulose (Sirviö, Hyväkkö, Liimatainen, Niinimäki, & Hormi, 2011), several recycling cycles can lead to accumulation of these salts in the solution, which can decrease reaction efficiency. Therefore, in the industrial process, it is necessary to either discard the oxidation solution or remove the salts.

Catalytic reactions could be used to avoid the consumption of toxic and costly chemicals such as periodate, but studies on the catalytic oxidation of polysaccharides to aldehydes are scarce. The problem in catalytic periodate oxidation might originate from the use of a strong oxidizing agent to generate periodate from iodate. The strong oxidation potential of periodate is indeed demonstrated in organic synthesis where it has been studied as a primary oxidant for catalytic oxidants (Zhou et al., 2013). In addition, as was discussed above, the regeneration of spent periodate is generally performed under strong alkaline conditions, which leads to the beta-elimination reaction and thus the degradation of polysaccharides. Furthermore, a stronger, less selective oxidation could lead to over-oxidation of the aldehyde functionality.

6. Discussion

Periodate oxidation of the various wood-based hierarchies has been reported to lead to functionalization and degradation, which results in oxidized hierarchies with smaller dimensions than the starting material (Chen & van de Ven, 2016; Errokh et al., 2018; Mendoza et al., 2019; Sirviö, Visanko, Laitinen et al., 2016; Sirviö, Hasa et al., 2015). However, the level of degradation is dependent on the DO, which depends on the oxidation conditions. The oxidant to substrate ratio defines the amount of aldehyde groups generated; increasing the temperature can boost this but with an increased chance of degradation (Liu et al., 2012; Sun et al., 2015).

The highest hierarchical level considered in this review is a *fiber* (Fig. 4). Preservation of the hierarchy of the fiber during oxidation requires mild conditions. However, its disintegration into smaller fragments at least to some extent seems to be inevitable based on findings in the literature. It is not necessarily the case that oxidation of one hierarchical level entails conversion into another; rather, the product is a mixture of different fractions. The generation of a water-soluble fraction is reported together with the generation of particulate fractions (Mendoza et al., 2019). The latter consisted of fibrils from the fiber cell wall and crystalline fractions (CNCs). Here, we categorize these materials into achievable *particulate oxidation hierarchies* (Fig. 4).

Often, the starting hierarchies for oxidation are those fibrils or crystals that are on a lower hierarchical level than fibers. Again, depending on the severity of the oxidation conditions, the initial hierarchy can be preserved to an extent or converted to a lower hierarchical level. This adds another group of oxidation products that consist of smaller molecular fragments. Hence, we add *molecular oxidation products* to our categorization of achievable oxidation hierarchies (Fig. 4).

The paradigm shift of utilizing periodate oxidation for materials engineering has brought about a reversal in the traversing of hierarchical ladders. Instead of descending from the higher (fiber) to the lower (particulate, molecular), the generated aldehyde functionality has been used for crosslinking the hierarchies (all levels) and typically leads to hierarchical ascent. These *regenerated oxidation products* comprise another category included in Fig. 4. These products are mostly papers (Larsson, Gimåker, & Wågberg, 2008; Strong et al., 2018; Sun et al., 2015; Wang et al., 2012; Zeronian et al., 1964), films (Kasai et al., 2014; Larsson & Wågberg, 2016; Nypelö et al., 2018), gels (Chinga-Carrasco & Syverud, 2014; Kim & Kuga, 2000; Köhnke et al., 2014; Plappert et al., 2019; Stratz et al., 2019), and composites (Codou et al., 2015; Zhang, Liu, Liu et al., 2019).

The mechanism of periodate oxidation remains contentious. The most disputed issue has been if the oxidation proceeds homogeneously or non-homogeneously. Identification of several phases of oxidation (Calvini & Gorassini, 2012; Liu et al., 2012; Potthast et al., 2007, 2009) complicates resolution on this. It has been suggested that oxidation starts in the amorphous regime of the starting material due to its higher reactivity (Liu et al., 2012). It continues by reacting on the edges/surfaces of the crystalline structures, and only strong oxidative environments reach the crystalline core. CNCs are notorious for their resistance to severe conditions, such as acid hydrolysis and solubilization. Wood fibers are also translated in other established processes into smaller fragments with already less harsh treatments, such as hot water or solvent extractions and mechanical treatments.

Accessibility studies are scarce, but an example can be given from a study on cotton fabrics where the oxidation indeed increased accessibility (Hao et al., 2018). Regarding crystal accessibility, intuitively, oxidant penetration into the crystal should be restricted. Indications of fragmentation of oxidized crystals into polymeric, oligomeric, and monomeric fractions support this hypothesis (Koso et al., 2020). The hypothesis that the surface peeling dominates the oxidation mechanism becomes appealing.

Complexity is added to the interpretation when considering that, at a high DO, dissolution into warm water can solubilize the oxidized hierarchies. The lack of in-situ analytics makes direct observation of the transition phases challenging. Then again, the diverse observations of changes in crystal dimensions, either thinner or shorter (Chen & van de Ven, 2016; Conley et al., 2016; Leguy et al., 2018), challenge the chemically intuitive assumption about the peeling reaction being the only contributor.

7. Concluding remarks

Periodate oxidation is a modification route specific for the diol structures in aqueous environment for polysaccharide materials. These advantages have made it a frequently applied modulator of chemical and physical properties of the polysaccharide materials. The last decade has seen publications reporting engineering of wood and polysaccharide

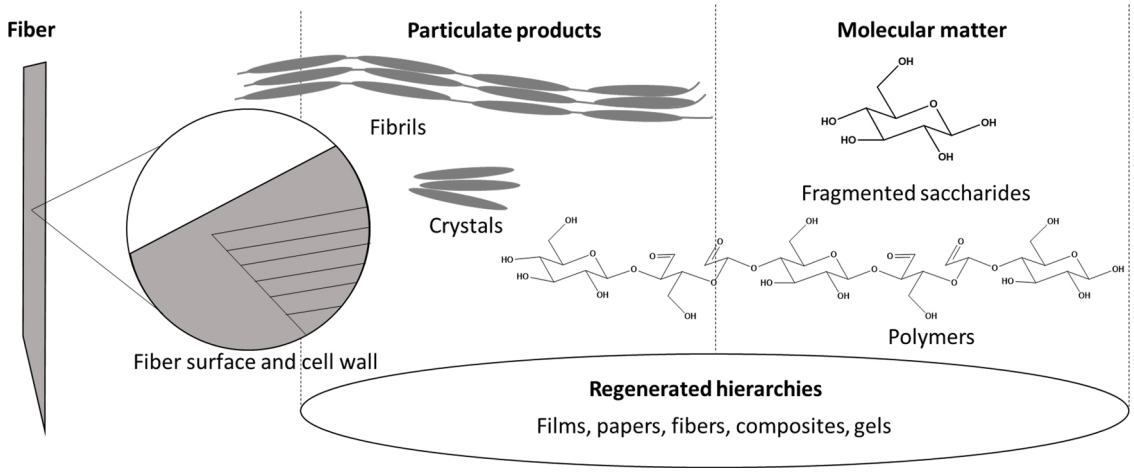

Fig. 4. Scheme of the modulated wood polysaccharide hierarchies by periodate oxidation. The highest hierarchical level (left) includes the fiber and fiber surface. Particulate products are mostly fibrils and crystals. Molecular matter comprises monosaccharides, oligosaccharides and polysaccharides. Regenerated hierarchies include papers, films, composites, and gels. Drawn by the authors with PowerPoint.

materials with periodate oxidation. The focus has clearly shifted from analytics to materials. Much effort has been put into elucidating the mechanism of periodate oxidation. However, it appears that the mechanism or the prospected hierarchy cannot be generalized; rather, it is a sum of the starting hierarchy and the oxidation conditions. Hence, mechanisms are case-by-case basis. We foresee that future research on this topic will progress in the direction of materials engineering, preserving fiber, fibril, and crystal structures while modifying the surfaces or shells of particulate matter. Utilization of crosslinking with the help of the surface or shell functionalities will be important.

Periodate oxidation is promising for several materials engineering applications such as modification of wood fibers to enable thermal processing, activation of cellulose particles for crosslinking to enable materials with higher strength than the individual components can provide, and reaction with substances that can bring functionality to cellulose for antibacterial properties, for sensing or for capture. The possibility of separating cellulose material in particle fractions with different dimensions is another intriguing opportunity. Successful alteration of the properties of raw materials signals a need for progress in process optimization as well. Recycling and recovery of reagents and solvents is a crucial step in the industrial process. The research we reviewed in Chapter 5 showed that the oxidation process, including recovery and recycling, is industrially applicable, yet the endeavor still requires academic and, especially, industrial attention.

CRediT authorship contribution statement

Tiina Nypelö: Conceptualization, Writing - original draft, Writing - review & editing. **Barbara Berke:** Writing - review & editing. **Stefan Spirk:** Writing - review & editing. **Juho Antti Sirviö:** Writing - review & editing.

Acknowledgements

The authors are thankful for the support of Treesearch through the Research Infrastructure access program. The Chalmers Material Analysis Laboratory (CMAL) is acknowledged for providing access to the measurements used for the crystallinity analysis. TN acknowledges the research groups of Anette Larsson, Anna Ström, and Merima Hasani for the many discussions on periodate oxidation of polysaccharides.

References

Abdel-Akher, M., Hamilton, J. K., Montgomery, R., & Smith, F. (1952). A new procedure for the determination of the fine structure of polysaccharides. *Journal of the American Chemical Society, 74*(19), 4970–4971.

Agarwal, U. P., Ralph, S. A., Reiner, R. S., Moore, R. K., & Baez, C. (2014). Impacts of fiber orientation and milling on observed crystallinity in jack pine. *Wood Science and Technology, 48*(6), 1213–1227.

Ahvenainen, P., Kontro, I., & Svedström, K. (2016). Comparison of sample crystallinity determination methods by X-ray diffraction for challenging cellulose I materials. *Cellulose, 23*(2), 1073–1086.

Alam, M. N., & Christopher, L. P. (2017). A novel, cost-effective and eco-friendly method for preparation of textile fibers from cellulosic pulps. *Carbohydrate Polymers, 173*, 253–258.

Amer, H., Nypelö, T., Sulaeva, I., Bacher, M., Henniges, U., Potthast, A., et al. (2016). Synthesis and characterization of periodate-oxidized polysaccharides: Dialdehyde xylan (DAX). *Biomacromolecules, 17*(9), 2972–2980.

Anastas, P., & Eghbali, N. (2010). Green chemistry: Principles and practice. *Chemical Society Reviews, 39*(1), 301–312.

Aspinall, G., & Ross, K. (1963). The degradation of two periodate-oxidised arabinoxylans. *Journal of the Chemical Society (Resumed)*, 1681–1686.

Avigad, G. (1969). Rapid, sensitive determination of periodate. *Carbohydrate Research, 11*(1), 119–123.

Azzam, F., Galliot, M., Putaux, J.-L., Heux, L., & Jean, B. (2015). Surface peeling of cellulose nanocrystals resulting from periodate oxidation and reductive amination with water-soluble polymers. *Cellulose, 22*(6), 3701–3714.

Babor, K., Kaláč, V., & Tihlaric, K. (1973). Periodate oxidation of saccharides. III. Comparison of the methods for determining the consumption of sodium periodate and the amount of formic acid formed. *Chemical Papers, 27*(5), 676–680.

Bansal, M., Chauhan, G. S., Kaushik, A., & Sharma, A. (2016). Extraction and functionalization of bagasse cellulose nanofibres to Schiff-base based antimicrobial membranes. *International Journal of Biological Macromolecules, 91*, 887–894.

Barroso, N., Costamagna, J., Matsuhiro, B., & Villagran, M. (1997). The xylan from Palmaria decipiens: Chemical modification and formation of a Cu (II). *Boletin de la Sociedad Chilena de Quimica, 42*(3), 301–306.

Bates, S., Zografi, G., Engers, D., Morris, K., Crowley, K., & Newman, A. (2006). Analysis of amorphous and nanocrystalline solids from their X-ray diffraction patterns. *Pharmaceutical Research, 23*(10), 2333–2349.

Bayani, S., Taghiyari, H. R., & Papadopoulos, A. N. (2019). Physical and mechanical properties of thermally-modified beech wood impregnated with silver nano-suspension and their relationship with the crystallinity of cellulose. *Polymers, 11*(10), 1538.

Besemer, A., 2003. Recovery process for spent periodate. Google Patents.

Bobbitt, J. (1956). Periodate oxidation of carbohydrates. *Advances in carbohydrate chemistry* (pp. 1–41). Elsevier.

Börjesson, M., Larsson, A., Westman, G., & Ström, A. (2018). Periodate oxidation of xylan-based hemicelluloses and its effect on their thermal properties. *Carbohydrate Polymers, 202*, 280–287.

Brauer, G. (2012). *Handbook of preparative inorganic chemistry*. Elsevier.

Calvini, P., & Gorassini, A. (2012). Surface and bulk reactions of cellulose oxidation by periodate. A simple kinetic model. *Cellulose, 19*(4), 1107–1114.

Cervin, N. T., Johansson, E., Larsson, P. A., & Wågberg, L. (2016). Strong, water-durable, and wet-resilient cellulose nanofibril-stabilized foams from oven drying. *ACS Applied Materials & Interfaces, 8*(18), 11682–11689.

Chemin, M., Rakotovelo, A., Ham-Pichavant, F., Chollet, G., da Silva Perez, D., Petit-Conil, M., et al. (2015). Synthesis and characterization of functionalized 4-O-methylglucuronoxylan derivatives. *Holzforschung, 69*(6), 713–720.

Chemin, M., Rakotovelo, A., Ham-Pichavant, F., Chollet, G., Da Silva Perez, D., Petit-Conil, M., et al. (2016). Periodate oxidation of 4-O-methylglucuronoxylans: Influence of the reaction conditions. *Carbohydrate Polymers, 142*, 45–50.
Chen, D., & van de Ven, T. G. (2016). Morphological changes of sterically stabilized nanocrystalline cellulose after periodate oxidation. *Cellulose, 23*(2), 1051–1059.
Chen, H., Sharma, S. K., Sharma, P. R., Yeh, H., Johnson, K., & Hsiao, B. S. (2019). Arsenic (iii) removal by nanostructured dialdehyde cellulose–cysteine microscale and nanoscale fibers. *ACS Omega, 4*(26), 22008–22020.
Chinga-Carrasco, G., & Syverud, K. (2014). Pretreatment-dependent surface chemistry of wood nanocellulose for pH-sensitive hydrogels. *Journal of Biomaterials Applications, 29*(3), 423–432.
Codou, A., Guigo, N., Heux, L., & Sbirrazzuoli, N. (2015). Partial periodate oxidation and thermal cross-linking for the processing of thermoset all-cellulose composites. *Composites Science and Technology, 117*, 54–61.
Conley, K., Whitehead, M., & van de Ven, T. G. (2016). Chemically peeling layers of cellulose nanocrystals by periodate and chlorite oxidation. *Cellulose, 23*(3), 1553–1563.
Coseri, S., Biliuta, G., Zemljič, L. F., Srndovic, J. S., Larsson, P. T., Strnad, S., et al. (2015). One-shot carboxylation of microcrystalline cellulose in the presence of nitroxyl radicals and sodium periodate. *RSC Advances, 5*(104), 85889–85897.
Dahlström, C., Durán, V. L., Keene, S., Salleo, A., Norgren, M., & Wågberg, L. (2020). Ion conductivity through TEMPO-mediated oxidated and periodate oxidated cellulose membranes. *Carbohydrate Polymers, 233*, Article 115829.
Dash, R., Foston, M., & Ragauskas, A. J. (2013). Improving the mechanical and thermal properties of gelatin hydrogels cross-linked by cellulose nanowhiskers. *Carbohydrate Polymers, 91*(2), 638–645.
Dryhurst, G. (2015). *Periodate oxidation of diol and other functional groups: Analytical and structural applications*. Elsevier.
Durán, V. L., Larsson, P. A., & Wågberg, L. (2016). On the relationship between fibre composition and material properties following periodate oxidation and borohydride reduction of lignocellulosic fibres. *Cellulose, 23*(6), 3495–3510.
Durán, V. L., Larsson, P. A., & Wågberg, L. (2018). Chemical modification of cellulose-rich fibres to clarify the influence of the chemical structure on the physical and mechanical properties of cellulose fibres and thereof made sheets. *Carbohydrate Polymers, 182*, 1–7.
Erlandsson, J., Pettersson, T., Ingverud, T., Granberg, H., Larsson, P. A., Malkoch, M., et al. (2018). On the mechanism behind freezing-induced chemical crosslinking in ice-templated cellulose nanofibril aerogels. *Journal of Materials Chemistry A, 6*(40), 19371–19380.
Errezma, M., Mabrouk, A. B., Magnin, A., Dufresne, A., & Boufi, S. (2018). Surfactant-free emulsion Pickering polymerization stabilized by aldehyde-functionalized cellulose nanocrystals. *Carbohydrate Polymers, 202*, 621–630.
Errokh, A., Magnin, A., Putaux, J.-L., & Boufi, S. (2018). Morphology of the nanocellulose produced by periodate oxidation and reductive treatment of cellulose fibers. *Cellulose, 25*(7), 3899–3911.
Ettenauer, M., Loth, F., Thummler, K., Fischer, S., Weber, V., & Falkenhagen, D. (2011). Characterization and functionalization of cellulose microbeads for extracorporeal blood purification. *Cellulose, 18*(5), 1257–1263.
French, A. D. (2020). Increment in evolution of cellulose crystallinity analysis. *Cellulose, 27*, 5445–5448.
Fu, G.-Q., Zhang, S.-C., Chen, G.-G., Hao, X., Bian, J., & Peng, F. (2020). Xylan-based hydrogels for potential skin care application. *International Journal of Biological Macromolecules, 158*, 244–250.
Garvey, C. J., Parker, I. H., & Simon, G. P. (2005). On the interpretation of X-ray diffraction powder patterns in terms of the nanostructure of cellulose I fibres. *Macromolecular Chemistry and Physics, 206*(15), 1568–1575.
Ge, H., Zhang, L., Xu, M., Cao, J., & Kang, C. (2016). Preparation of dialdehyde cellulose and its antibacterial activity. *International Conference on Applied Biotechnology*, 545–553. Springer.
Goldfinger, G., Mark, H., & Siggia, S. (1943). Kinetics of oxidation of cellulose with periodic acid. *Industrial and Engineering Chemistry, 35*(10), 1083–1086.
Gorur, Y. C., Larsson, P. A., & Wågberg, L. (2020). Self-fibrillating cellulose fibers: Rapid in situ nanofibrillation to prepare strong, transparent, and gas barrier nanopapers. *Biomacromolecules, 21*(4), 1480–1488.
Guigo, N., Mazeau, K., Putaux, J.-L., & Heux, L. (2014). Surface modification of cellulose microfibrils by periodate oxidation and subsequent reductive amination with benzylamine: A topochemical study. *Cellulose, 21*(6), 4119–4133.
Guthrie, R. (1962). The "dialdehydes" from the periodate oxidation of carbohydrates. *Advances in carbohydrate chemistry* (pp. 105–158). Elsevier.
Hao, L., Wang, R., Zhao, Y., Fang, K., & Cai, Y. (2018). The enzymatic actions of cellulase on periodate oxidized cotton fabrics. *Cellulose, 25*(11), 6759–6769.
Hashem, M. A., Elnagar, M. M., Kenawy, I. M., & Ismail, M. A. (2020). Synthesis and application of hydrazono-imidazoline modified cellulose for selective separation of precious metals from geological samples. *Carbohydrate Polymers*, Article 116177.
Hay, G., Lewis, B. A., & Smith, F. (1965). Periodate oxidation of polysaccharides: General procedures. *Methods in Carbohydrate Chemistry, 5*(3), 5.
He, J., Cui, S., & Wang, S. Y. (2008). Preparation and crystalline analysis of high-grade bamboo dissolving pulp for cellulose acetate. *Journal of Applied Polymer Science, 107*(2), 1029–1038.
Heinze, T., Koschella, A., & Ebringerova, A. (2004). Chemical functionalization of xylan: A short review. *ACS Symposium Series, 864*, 312–325. Washington, DC; American Chemical Society; 1999.
Hell, S., Ohkawa, K., Amer, H., Potthast, A., & Rosenau, T. (2018). "Dialdehyde cellulose" nanofibers by electrospinning as polyvinyl alcohol blends: Manufacture and product characterization. *Journal of Wood Chemistry and Technology, 38*(2), 96–110.
Henschen, J., Larsson, P. A., Illergård, J., Ek, M., & Wågberg, L. (2017). Bacterial adhesion to polyvinylamine-modified nanocellulose films. *Colloids and Surfaces B: Biointerfaces, 151*, 224–231.
Hollertz, R., Durán, V. L., Larsson, P. A., & Wågberg, L. (2017). Chemically modified cellulose micro-and nanofibrils as paper-strength additives. *Cellulose, 24*(9), 3883–3899.
Hou, Q., Liu, W., Liu, Z., & Bai, L. (2007). Characteristics of wood cellulose fibers treated with periodate and bisulfite. *Industrial & Engineering Chemistry Research, 46*(23), 7830–7837.
Huang, B., He, H., Liu, H., Zhang, Y., Peng, X., & Wang, B. (2020). Multi-type cellulose nanocrystals from sugarcane bagasse and their nanohybrids constructed with polyhedral oligomeric silsesquioxane. *Carbohydrate Polymers, 227*, Article 115368.
Hult, E.-L., Iversen, T., & Sugiyama, J. (2003). Characterization of the supermolecular structure of cellulose in wood pulp fibres. *Cellulose, 10*(2), 103–110.
Hurd, C. D. (1966). Hemiacetals, aldals and hemialdals. *Journal of Chemical Education, 43*(10), 527.
Imamura, A. H., Segato, T. P., de Oliveira, L. J. M., Hassan, A., Crespilho, F. N., & Carrilho, E. (2020). Monitoring cellulose oxidation for protein immobilization in paper-based low-cost biosensors. *Microchimica et Ichnoanalytica Acta, 187*(272), 1–8.
Isobe, N., Lee, D.-S., Kwon, Y.-J., Kimura, S., Kuga, S., Wada, M., et al. (2011). Immobilization of protein on cellulose hydrogel. *Cellulose, 18*(5), 1251.
Janssen, L., & Blijlevens, M. (2003). Electrochemical oxidation of iodate to periodate. *Electrochimica Acta, 48*(25–26), 3959–3964.
Ji, Y., Xu, Q., Jin, L., & Fu, Y. (2020). Cellulosic paper with high antioxidative and barrier properties obtained through incorporation of tannin into kraft pulp fibers. *International Journal of Biological Macromolecules, 162*, 678–684.
Jin, L. Q., Li, W. G., Xu, Q. H., & Sun, Q. C. (2015). Amino-functionalized nanocrystalline cellulose as an adsorbent for anionic dyes. *Cellulose, 22*(4), 2443–2456.
Jones, A. O. F., Resel, R., Schrode, B., Machado-Charry, E., Rothel, C., Kunert, B., et al. (2020). Structural order in cellulose thin films prepared from a trimethylsilyl precursor. *Biomacromolecules, 21*(2), 653–659.
Kasai, W., Morooka, T., & Ek, M. (2014). Mechanical properties of films made from dialcohol cellulose prepared by homogeneous periodate oxidation. *Cellulose, 21*(1), 769–776.
Kekäläinen, K., Liimatainen, H., & Niinimäki, J. (2014). Disintegration of periodate–chlorite oxidized hardwood pulp fibres to cellulose microfibrils: Kinetics and charge threshold. *Cellulose, 21*(5), 3691–3700.
Keshk, S. M., Bondock, S., El-Zahhar, A. A., & Haija, M. A. (2019). Synthesis and characterization of novel Schiff's bases derived from dialdehyde cellulose-6-phosphate. *Cellulose, 26*(6), 3703–3712.
Kesselmans, R., & Peter, W. (1996). A method for the oxidation of starch with periodate. *WO, 98*(271), 19.
Khalil, H. A., Davoudpour, Y., Islam, M. N., Mustapha, A., Sudesh, K., Dungani, R., et al. (2014). Production and modification of nanofibrillated cellulose using various mechanical processes: A review. *Carbohydrate Polymers, 99*, 649–665.
Kim, J. Y., & Choi, H.-M. (2014). Cationization of periodate-oxidized cotton cellulose with choline chloride. *Cellul Chem Technol, 48*(1–2), 25–32.
Kim, U. J., & Kuga, S. (2000). Reactive interaction of aromatic amines with dialdehyde cellulose gel. *Cellulose, 7*(3), 287–297.
Kim, U.-J., Wada, M., & Kuga, S. (2004). Solubilization of dialdehyde cellulose by hot water. *Carbohydrate Polymers, 56*(1), 7–10.
Kim, U. J., Kuga, S., Wada, M., Okano, T., & Kondo, T. (2000). Periodate oxidation of crystalline cellulose. *Biomacromolecules, 1*(3), 488–492.
Kochumalayil, J. J., Zhou, Q., Kasai, W., & Berglund, L. A. (2013). Regioselective modification of a xyloglucan hemicellulose for high-performance biopolymer barrier films. *Carbohydrate Polymers, 93*(2), 466–472.
Köhnke, T., Elder, T., Theliander, H., & Ragauskas, A. J. (2014). Ice templated and cross-linked xylan/nanocrystalline cellulose hydrogels. *Carbohydrate Polymers, 100*, 24–30.
Konduri, M. (2017). New generation of dispersants by grafting lignin or xylan. *Doctoral dissertation*. Lakehead University.
Kontturi, E., & Spirk, S. (2019). Ultrathin films of cellulose: A materials perspective. *Frontiers in Chemistry, 7*, 488.
Koprivica, S., Siller, M., Hosoya, T., Roggenstein, W., Rosenau, T., & Potthast, A. (2016). Regeneration of aqueous periodate solutions by ozone treatment: A sustainable approach for dialdehyde cellulose production. *ChemSusChem, 9*(8), 825–833.
Koso, T., Rico del Cerro, D., Heikkinen, S., Nypelö, T., Buffiere, J., Perea-Buceta, J. E., et al. (2020). Quantitative HSQC in the analysis of celluloses and oxidized celluloses using solution-state NMR in the [P4444][OAc]:DMSO-d6 electrolyte. *Cellulose, 27*, 7929–7953.
Kriechbaum, K., & Bergström, L. (2020). Antioxidant and UV-blocking leather-inspired nanocellulose-based films with high wet strength. *Biomacromolecules, 21*(5), 1720–1728.
Kristiansen, K. A., Potthast, A., & Christensen, B. E. (2010). Periodate oxidation of polysaccharides for modification of chemical and physical properties. *Carbohydrate Research, 345*(10), 1264–1271.
Kumari, S., Mankotia, D., & Chauhan, G. S. (2016). Crosslinked cellulose dialdehyde for Congo red removal from its aqueous solutions. *Journal of Environmental Chemical Engineering, 4*(1), 1126–1136.
Kwak, H. W., Lee, H., Park, S., Lee, M. E., & Jin, H.-J. (2020). Chemical and physical reinforcement of hydrophilic gelatin film with di-aldehyde nanocellulose. *International Journal of Biological Macromolecules, 146*, 332–342.
Laitinen, O., Hartmann, R., Sirviö, J. A., Liimatainen, H., Rudolph, M., Ämmälä, A., et al. (2016). Alkyl aminated nanocelluloses in selective flotation of aluminium oxide and quartz. *Chemical Engineering Science, 144*, 260–266.

Laitinen, O., Kemppainen, K., Ämmälä, A., Sirviö, J. A., Liimatainen, H., & Niinimäki, J. (2014). Use of chemically modified nanocelluloses in flotation of hematite and quartz. *Industrial & Engineering Chemistry Research, 53*(52), 20092–20098.
Larsson, P. A., Gimåker, M., & Wågberg, L. (2008). The influence of periodate oxidation on the moisture sorptivity and dimensional stability of paper. *Cellulose, 15*(6), 837–847.
Larsson, P. A., Kochumalayil, J. J., & Wågberg, L. (2013). Oxygen and water vapour barrier films with low moisture sensitivity fabricated from self-cross-linking fibrillated cellulose. *15th fundamental research symposium: advances in pulp and paper research*, 851–866.
Larsson, P. A., Berglund, L. A., & Wågberg, L. (2014a). Highly ductile fibres and sheets by core-shell structuring of the cellulose nanofibrils. *Cellulose, 21*(1), 323–333.
Larsson, P. A., Berglund, L. A., & Wågberg, L. (2014b). Ductile all-cellulose nanocomposite films fabricated from core–shell structured cellulose nanofibrils. *Biomacromolecules, 15*(6), 2218–2223.
Larsson, P. A., Pettersson, T., & Wågberg, L. (2014). Improved barrier films of cross-linked cellulose nanofibrils: A microscopy study. *Green Materials, 2*(4), 163–168.
Larsson, P. A., & Wågberg, L. (2016). Towards natural-fibre-based thermoplastic films produced by conventional papermaking. *Green Chemistry, 18*(11), 3324–3333.
Leguy, J., Diallo, A., Putaux, J.-L., Nishiyama, Y., Heux, L., & Jean, B. (2018). Periodate oxidation followed by NaBH4 reduction converts microfibrillated cellulose into sterically stabilized neutral cellulose nanocrystal suspensions. *Langmuir, 34*(37), 11066–11075.
Li, W., Ju, B., & Zhang, S. (2019). Preparation of cysteamine-modified cellulose nanocrystal adsorbent for removal of mercury ions from aqueous solutions. *Cellulose, 26*(8), 4971–4985.
Li, W., Ju, B., & Zhang, S. (2020). Novel amphiphilic cellulose nanocrystals for pH-responsive Pickering emulsions. *Carbohydrate Polymers, 229*, Article 115401.
Li, J., Kang, L., Wang, B., Chen, K., Tian, X., Ge, Z., et al. (2018). Controlled release and long-term antibacterial activity of dialdehyde nanofibrillated cellulose/silver nanoparticle composites. *ACS Sustainable Chemistry & Engineering, 7*(1), 1146–1158.
Li, Z., Shao, L., Hu, W., Zheng, T., Lu, L., Cao, Y., et al. (2018). Excellent reusable chitosan/cellulose aerogel as an oil and organic solvent absorbent. *Carbohydrate Polymers, 191*, 183–190.
Liimatainen, H., Sirviö, J., Pajari, H., Hormi, O., & Niinimäki, J. (2013). Regeneration and recycling of aqueous periodate solution in dialdehyde cellulose production. *Journal of Wood Chemistry and Technology, 33*(4), 258–266.
Liimatainen, H., Visanko, M., Sirviö, J. A., Hormi, O. E., & Niinimäki, J. (2012). Enhancement of the nanofibrillation of wood cellulose through sequential periodate–chlorite oxidation. *Biomacromolecules, 13*(5), 1592–1597.
Lindh, J., Carlsson, D. O., Strømme, M., & Mihranyan, A. (2014). Convenient one-pot formation of 2, 3-dialdehyde cellulose beads via periodate oxidation of cellulose in water. *Biomacromolecules, 15*(5), 1928–1932.
Lindh, J., Ruan, C., Strømme, M., & Mihranyan, A. (2016). Preparation of porous cellulose beads via introduction of diamine spacers. *Langmuir, 32*(22), 5600–5607.
Linvill, E., Larsson, P. A., & Östlund, S. (2017). Advanced three-dimensional paper structures: Mechanical characterization and forming of sheets made from modified cellulose fibers. *Materials & Design, 128*, 231–240.
Lipniunas, P., Angel, A.-S., Erlansson, K., Lindh, F., & Nilsson, B. (1992). Mass spectrometry of high-mannose oligosaccharides after trifluoroacetolysis and periodate oxidation. *Analytical Biochemistry, 200*(1), 58–67.
Liu, P., Mai, C., & Zhang, K. (2017). Formation of uniform multi-stimuli-responsive and multiblock hydrogels from dialdehyde cellulose. *ACS Sustainable Chemistry & Engineering, 5*(6), 5313–5319.
Liu, P., Pang, B., Dechert, S., Zhang, X., Andreas, L., Fischer, S., et al. (2019). Structure selectivity of alkaline periodate oxidation on lignocellulose for facile isolation of cellulose nanocrystals. *Angewandte Chemie (International Ed in English), 59*(8), 3218–3225.
Liu, P., Pang, B., Tian, L., Schäfer, T., Gutmann, T., Liu, H., et al. (2018). Efficient, self-terminating isolation of cellulose nanocrystals through periodate oxidation in Pickering emulsions. *ChemSusChem, 11*(20), 3581–3585.
Liu, X., Wang, L., Song, X., Song, H., Zhao, J. R., & Wang, S. (2012). A kinetic model for oxidative degradation of bagasse pulp fiber by sodium periodate. *Carbohydrate Polymers, 90*(1), 218–223.
Lucia, A., Bacher, M., van Herwijnen, H. W., & Rosenau, T. (2020). A direct silanization protocol for dialdehyde cellulose. *Molecules, 25*(10), 2458.
Luo, X., Xia, J., Jiang, X., Yang, M., & Liu, S. (2019). Cellulose-based strips designed based on a sensitive enzyme colorimetric assay for the low concentration of glucose detection. *Analytical Chemistry, 91*(24), 15461–15468.
Lv, M., Ma, X., Anderson, D. P., & Chang, P. R. (2018). Immobilization of urease onto cellulose spheres for the selective removal of urea. *Cellulose, 25*(1), 233–243.
Madivoli, E. S., Kareru, P. G., Gachanja, A. N., Mugo, S. M., & Makhanu, D. S. (2019). Synthesis and characterization of dialdehyde cellulose nanofibers from O. sativa husks. *SN Applied Sciences, 1*(7), 723.
Malaprade, L. (1928). Oxidation of some polyalcohols by periodic acid—Applications. *Comptes Rendus, 186*, 382–384.
Matsumura, S., Nishioka, M., & Yoshikawa, S. (1991). Enzymatically degradable poly (carboxylic acid) derived from polysaccharide. *Die Makromolekulare Chemie Rapid Communications, 12*(2), 89–94.
Mendoza, D. J., Browne, C., Raghuwanshi, V. S., Simon, G. P., & Garnier, G. (2019). One-shot TEMPO-periodate oxidation of native cellulose. *Carbohydrate Polymers, 226*, Article 115292.
Meyer, K. H., & Misch, L. (1937). Positions des atomes dans le nouveau modele spatial de la cellulose. *Helvetica Chimica Acta, 20*(1), 232–244.
Mohamed, A. L., Hassabo, A. G., Shaarawy, S., & Hebeish, A. (2017). Benign development of cotton with antibacterial activity and metal sorpability through introduction amino triazole moieties and AgNPs in cotton structure pre-treated with periodate. *Carbohydrate Polymers, 178*, 251–259.
Morooka, T., Norimoto, M., & Yamada, T. (1989). Periodate oxidation of cellulose by homogeneous reaction. *Journal of Applied Polymer Science, 38*(5), 849–858.
Mou, K., Li, J., Wang, Y., Cha, R., & Jiang, X. (2017). 2,3-Dialdehyde nanofibrillated cellulose as a potential material for the treatment of MRSA infection. *Journal of Materials Chemistry B, 5*(38), 7876–7884.
Münster, L., Vícha, J., Klofáč, J., Masař, M., Kucharczyk, P., & Kuřitka, I. (2017). Stability and aging of solubilized dialdehyde cellulose. *Cellulose, 24*(7), 2753–2766.
Nechyporchuk, O., Belgacem, M. N., & Bras, J. (2016). Production of cellulose nanofibrils: A review of recent advances. *Industrial Crops and Products, 93*, 2–25.
Nelson, M. L., & O'Connor, R. T. (1964a). Relation of certain infrared bands to cellulose crystallinity and crystal lattice type. Part II. A new infrared ratio for estimation of crystallinity in celluloses I and II. *Journal of Applied Polymer Science, 8*(3), 1325–1341.
Nelson, M. L., & O'Connor, R. T. (1964b). Relation of certain infrared bands to cellulose crystallinity and crystal latticed type. Part I. Spectra of lattice types I, II, III and of amorphous cellulose. *Journal of Applied Polymer Science, 8*(3), 1311–1324.
Nikolic, T., Kostic, M., Praskalo, J., Pejic, B., Petronijevic, Z., & Skundric, P. (2010). Sodium periodate oxidized cotton yarn as carrier for immobilization of trypsin. *Carbohydrate Polymers, 82*(3), 976–981.
Nishiyama, Y., Kim, U. J., Kim, D. Y., Katsumata, K. S., May, R. P., & Langan, P. (2003). Periodic disorder along ramie cellulose microfibrils. *Biomacromolecules, 4*(4), 1013–1017.
Noorian, S. A., Hemmatinejad, N., & Navarro, J. A. (2019). Ligand modified cellulose fabrics as support of zinc oxide nanoparticles for UV protection and antimicrobial activities. *International Journal of Biological Macromolecules, 154*, 1215–1226.
Nypelö, T., Amer, H., Konnerth, J., Potthast, A., & Rosenau, T. (2018). Self-standing nanocellulose Janus-type films with aldehyde and carboxyl functionalities. *Biomacromolecules, 19*(3), 973–979.
Ojala, J., Sirviö, J. A., & Liimatainen, H. (2016). Nanoparticle emulsifiers based on bifunctionalized cellulose nanocrystals as marine diesel oil–water emulsion stabilizers. *Chemical Engineering Journal, 288*, 312–320.
Ojala, J., Sirviö, J. A., & Liimatainen, H. (2018). Preparation of cellulose nanocrystals from lignin-rich reject material for oil emulsification in an aqueous environment. *Cellulose, 25*(1), 293–304.
Painter, T., & Larsen, B. (1970). Transient hemiacetal structures formed during the periodate oxidation of xylan. *Acta Chemica Scandinavica, 24*(7).
Park, S., Baker, J. O., Himmel, M. E., Parilla, P. A., & Johnson, D. K. (2010). Cellulose crystallinity index: Measurement techniques and their impact on interpreting cellulase performance. *Biotechnology for Biofuels, 3*(1).
Peng, X., Liu, P., Pang, B., Yao, Y., Wang, J., & Zhang, K. (2019). Facile fabrication of pH-responsive nanoparticles from cellulose derivatives via Schiff base formation for controlled release. *Carbohydrate Polymers, 216*, 113–118.
Pfeifer, V., Sohns, V., Conway, H., Lancaster, E., Dabic, S., & Griffin, E. (1960). Two stage process for dialdehyde starch using electrolytic regeneration of periodic acid. *Industrial and Engineering Chemistry, 52*(3), 201–206.
Pietrucha, K., & Safandowska, M. (2015). Dialdehyde cellulose-crosslinked collagen and its physicochemical properties. *Process Biochemistry, 50*(12), 2105–2111.
Plappert, S. F., Liebner, F. W., Konnerth, J., & Nedelec, J.-M. (2019). Anisotropic nanocellulose gel–membranes for drug delivery: Tailoring structure and interface by sequential periodate–chlorite oxidation. *Carbohydrate Polymers, 226*, Article 115306.
Plappert, S. F., Quraishi, S., Pircher, N., Mikkonen, K. S., Veigel, S., Klinger, K. M., et al. (2018). Transparent, flexible, and strong 2, 3-dialdehyde cellulose films with high oxygen barrier properties. *Biomacromolecules, 19*(7), 2969–2978.
Pommerening, K., Rein, H., Bertram, D., & Muller, R. (1992). Estimation of dialdehyde groups in 2,3-dialdehyde bead-cellulose. *Carbohydrate Research, 233*, 219–223.
Potthast, A., Kostic, M., Schiehser, S., Kosma, P., & Rosenau, T. (2007). Studies on oxidative modifications of cellulose in the periodate system: Molecular weight distribution and carbonyl group profiles. *Holzforschung, 61*(6), 662–667.
Potthast, A., Schiehser, S., Rosenau, T., & Kostic, M. (2009). Oxidative modifications of cellulose in the periodate system–reduction and beta-elimination reactions 2nd ICC 2007, Tokyo, Japan, October 25–29, 2007. *Holzforschung, 63*(1), 12–17.
PubChem Database. Sodium iodate, https://pubchem.ncbi.nlm.nih.gov/compound/Sodium-iodate (accessed on June 13, 2020).
PubChem Database. Sodium periodate, https://pubchem.ncbi.nlm.nih.gov/compound/Sodium-periodate (accessed on June 13, 2020).
Rajalaxmi, D., Jiang, N., Leslie, G., & Ragauskas, A. J. (2010). Synthesis of novel water-soluble sulfonated cellulose. *Carbohydrate Research, 345*(2), 284–290.
Rees, A., Powell, L. C., Chinga-Carrasco, G., Gethin, D. T., Syverud, K., Hill, K. E., et al. (2015). 3D bioprinting of carboxymethylated-periodate oxidized nanocellulose constructs for wound dressing applications. *BioMed Research International*, 925757.
Rietveld, H. (1969). A profile refinement method for nuclear and magnetic structures. *Journal of Applied Crystallography, 2*(2), 65–71.
Röder, T., Moosbauer, J., Fasching, M., Bohn, A., Fink, H.-P., Baldinger, T., et al. (2006). Crystallinity determination of native cellulose-comparison of analytical methods. *Lenzinger Berichte, 86*.
Rodrigues Filho, G., de Assunçao, R. M., Vieira, J. G., Meireles, C.d. S., Cerqueira, D. A., et al. (2007). Characterization of methylcellulose produced from sugar cane bagasse cellulose: Crystallinity and thermal properties. *Polymer Degradation and Stability, 92*(2), 205–210.
Röhrling, J., Potthast, A., Rosenau, T., Lange, T., Borgards, A., Sixta, H., et al. (2002). A novel method for the determination of carbonyl groups in cellulosics by fluorescence labeling. 2. Validation and applications. *Biomacromolecules, 3*(5), 969–975.

Rostami, J., Mathew, A. P., & Edlund, U. (2019). Zwitterionic acetylated cellulose nanofibrils. *Molecules, 24*(17), 3147.
Ruan, C.-Q., Strømme, M., & Lindh, J. (2018). Preparation of porous 2,3-dialdehyde cellulose beads crosslinked with chitosan and their application in adsorption of Congo red dye. *Carbohydrate Polymers, 181*, 200–207.
Sajid, M. S., Jabeen, F., Hussain, D., Gardner, Q. T. A. A., Ashiq, M. N., & Najam-ul-Haq, M. (2020). Boronic acid functionalized fibrous cellulose for the selective enrichment of glycopeptides. *Journal of Separation Science, 43*(7), 1348–1355.
Salama, A., Shukry, N., El-Gendy, A., & El-Sakhawy, M. (2017). Bioactive cellulose grafted soy protein isolate towards biomimetic calcium phosphate mineralization. *Industrial Crops and Products, 95*, 170–174.
Salmén, L., & Larsson, P. A. (2018). On the origin of sorption hysteresis in cellulosic materials. *Carbohydrate Polymers, 182*, 15–20.
Sedri, A., Naeimi, A., & Mohammadi, S. Z. (2018). An innovative synthesis of MoO3/Ag nanocomposite and catalytic application of immobilized molybdenum complex on cellulose extracting from Carthamus tinctorius. *Carbohydrate Polymers, 199*, 236–243.
Segal, L., Creely, J., Martin, A., Jr, & Conrad, C. (1959). An empirical method for estimating the degree of crystallinity of native cellulose using the X-ray diffractometer. *Textile Research Journal, 29*(10), 786–794.
Shaikh, H., Adsul, M., Gokhale, D., & Varma, A. (2011). Enhanced enzymatic hydrolysis of cellulose by partial modification of its chemical structure. *Carbohydrate Polymers, 86*(2), 962–968.
Sheikhi, A., & van de Ven, T. G. (2017). Colloidal aspects of Janus-like hairy cellulose nanocrystalloids. *Current Opinion in Colloid & Interface Science, 29*, 21–31.
Siller, M., Amer, H., Bacher, M., Roggenstein, W., Rosenau, T., & Potthast, A. (2015). Effects of periodate oxidation on cellulose polymorphs. *Cellulose, 22*(4), 2245–2261.
Široký, J., Blackburn, R. S., Bechtold, T., Taylor, J., & White, P. (2010). Attenuated total reflectance Fourier-transform Infrared spectroscopy analysis of crystallinity changes in lyocell following continuous treatment with sodium hydroxide. *Cellulose, 17*(1), 103–115.
Sirviö, J., Hyväkkö, U., Liimatainen, H., Niinimäki, J., & Hormi, O. (2011). Periodate oxidation of cellulose at elevated temperatures using metal salts as cellulose activators. *Carbohydrate Polymers, 83*(3), 1293–1297.
Sirviö, J. A., Liimatainen, H., Visanko, M., & Niinimäki, J. (2014). Optimization of dicarboxylic acid cellulose synthesis: Reaction stoichiometry and role of hypochlorite scavengers. *Carbohydrate Polymers, 114*, 73–77.
Sirviö, J. A., Hasa, T., Ahola, J., Liimatainen, H., Niinimäki, J., & Hormi, O. (2015). Phosphonated nanocelluloses from sequential oxidative–reductive treatment—Physicochemical characteristics and thermal properties. *Carbohydrate Polymers, 133*, 524–532.
Sirviö, J. A., Honkaniemi, S., Visanko, M., & Liimatainen, H. (2015). Composite films of poly (vinyl alcohol) and bifunctional cross-linking cellulose nanocrystals. *ACS Applied Materials & Interfaces, 7*(35), 19691–19699.
Sirviö, J. A., Visanko, M., Heiskanen, J. P., & Liimatainen, H. (2016). UV-absorbing cellulose nanocrystals as functional reinforcing fillers in polymer nanocomposite films. *Journal of Materials Chemistry A, 4*(17), 6368–6375.
Sirviö, J. A., Visanko, M., Laitinen, O., Ämmälä, A., & Liimatainen, H. (2016). Amino-modified cellulose nanocrystals with adjustable hydrophobicity from combined regioselective oxidation and reductive amination. *Carbohydrate Polymers, 136*, 581–587.
Song, K., Xu, H., Xie, K., & Yang, Y. (2017). Keratin-based biocomposites reinforced and cross-linked with dual-functional cellulose nanocrystals. *ACS Sustainable Chemistry & Engineering, 5*(7), 5669–5678.
Spedding, H. (1960). 628. Infrared spectra of periodate-oxidised cellulose. *Journal of the Chemical Society (Resumed)*, 3147–3152.
Stratz, J., Liedmann, A., Trutschel, M. L., Mader, K., Groth, T., & Fischer, S. (2019). Development of hydrogels based on oxidized cellulose sulfates and carboxymethyl chitosan. *Cellulose, 26*(12), 7371–7382.
Strong, E. B., Kirschbaum, C. W., Martinez, A. W., & Martinez, N. W. (2018). Paper miniaturization via periodate oxidation of cellulose. *Cellulose, 25*(6), 3211–3217.
Strong, E. B., Schultz, S. A., Martinez, A. W., & Martinez, N. W. (2019). Fabrication of miniaturized paper-based microfluidic devices (MicroPADs). *Scientific Reports, 1*, 1–9.
Sulaeva, I., Klinger, K. M., Amer, H., Henniges, U., Rosenau, T., & Potthast, A. (2015). Determination of molar mass distributions of highly oxidized dialdehyde cellulose by size exclusion chromatography and asymmetric flow field-flow fractionation. *Cellulose, 22*(6), 3569–3581.
Sun, B., Hou, Q. X., Liu, Z. H., & Ni, Y. H. (2015). Sodium periodate oxidation of cellulose nanocrystal and its application as a paper wet strength additive. *Cellulose, 22*(2), 1135–1146.
Sun, F., Liu, W., Dong, Z., & Deng, Y. (2017). Underwater superoleophobicity cellulose nanofibril aerogel through regioselective sulfonation for oil/water separation. *Chemical Engineering Journal, 330*, 774–782.
Teeäär, R., Serimaa, R., & Paakkari, T. (1987). Crystallinity of cellulose, as determined by CP/MAS NMR and XRD methods. *Polymer Bulletin, 17*(3), 231–237.
Terinte, N., Ibbett, R., & Schuster, K. C. (2011). Overview on native cellulose and microcrystalline cellulose I structure studied by X-ray diffraction (WAXD): Comparison between measurement techniques. *Lenzinger Berichte, 89*(1), 118–131.
Thygesen, A., Oddershede, J., Lilholt, H., Thomsen, A. B., & Ståhl, K. (2005). On the determination of crystallinity and cellulose content in plant fibres. *Cellulose, 12*(6), 563.
Tian, X., & Jiang, X. (2018). Preparing water-soluble 2, 3-dialdehyde cellulose as a bio-origin cross-linker of chitosan. *Cellulose, 25*(2), 987–998.
Tummalapalli, M., & Gupta, B. (2015). A UV-vis spectrophotometric method for the estimation of aldehyde groups in periodate-oxidized polysaccharides using 2, 4-dinitrophenyl hydrazine. *Journal of Carbohydrate Chemistry, 34*(6), 338–348.
Van De Ven, T. G., & Sheikhi, A. (2016). Hairy cellulose nanocrystalloids: A novel class of nanocellulose. *Nanoscale, 8*(33), 15101–15114.
Varma, A., & Kulkarni, M. (2002). Oxidation of cellulose under controlled conditions. *Polymer Degradation and Stability, 77*(1), 25–27.
Vicini, S., Princi, E., Luciano, G., Franceschi, E., Pedemonte, E., Oldak, D., et al. (2004). Thermal analysis and characterisation of cellulose oxidised with sodium methaperiodate. *Thermochimica Acta, 418*(1–2), 123–130.
Wang, S., Ge, L., Song, X., Yan, M., Ge, S., Yu, J., et al. (2012). Simple and covalent fabrication of a paper device and its application in sensitive chemiluminescence immunoassay. *Analyst, 137*(16), 3821–3827.
Xiao, G., Wang, Y., Zhang, H., Chen, L., & Fu, S. (2019). Facile strategy to construct a self-healing and biocompatible cellulose nanocomposite hydrogel via reversible acylhydrazone. *Carbohydrate Polymers, 218*, 68–77.
Xing, L., Gu, J., Zhang, W., Tu, D., & Hu, C. (2018). Cellulose I and II nanocrystals produced by sulfuric acid hydrolysis of Tetra pak cellulose I. *Carbohydrate Polymers, 192*, 184–192.
Xu, Q., Jin, L., Wang, Y., Chen, H., & Qin, M. (2019). Synthesis of silver nanoparticles using dialdehyde cellulose nanocrystal as a multi-functional agent and application to antibacterial paper. *Cellulose, 26*, 1309–1321.
Xu, Y., Shi, Y., Lei, F., & Dai, L. (2020). A novel and green cellulose-based Schiff base-Cu (II) complex and its excellent antibacterial activity. *Carbohydrate Polymers, 230*, Article 115671.
Xu, Q., Ji, Y., Sun, Q., Fu, Y., Xu, Y., & Jin, L. (2019). Fabrication of cellulose nanocrystal/chitosan hydrogel for controlled drug release. *Nanomaterials, 9*(2), 253.
Xu, Y. H., & Huang, C. (2011). Effect of sodium periodate selective oxidation on crystallinity of cotton cellulose. *Advanced Materials Research, 197*, 1201–1204.
Yan, G., Zhang, X., Li, M., Zhao, X., Zeng, X., Sun, Y., et al. (2018). Stability of soluble dialdehyde cellulose and the formation of hollow microspheres: Optimization and characterization. *ACS Sustainable Chemistry & Engineering, 7*(2), 2151–2159.
Yang, H., & van de Ven, T. G. (2016). Preparation of hairy cationic nanocrystalline cellulose. *Cellulose, 23*(3), 1791–1801.
Yang, H., Tejado, A., Alam, N., Antal, M., & van de Ven, T. G. (2012). Films prepared from electrosterically stabilized nanocrystalline cellulose. *Langmuir, 28*(20), 7834–7842.
Yao, M., Wang, Z., Liu, Y., Yang, G., & Chen, J. (2019). Preparation of dialdehyde cellulose graftead graphene oxide composite and its adsorption behavior for heavy metals from aqueous solution. *Carbohydrate Polymers, 212*, 345–351.
Yao, W., Weng, Y., & Catchmark, J. M. (2020). Improved cellulose X-ray diffraction analysis using Fourier series modeling. *Cellulose, 27*, 5563–5579.
Yuldoshov, S., Atakhanov, A., & Rashidova, S. (2016). Cotton cellulose, microcrystalline cellulose and nanocellulose: Carboxymethylation and oxidation reaction activity. *Journal of Nanoscience and Nanotechnology, 10*(6), 106.
Zeronian, S., Hudson, F., & Peters, R. (1964). The mechanical properties of paper made from periodate oxycellulose pulp and from the same pulp after reduction with borohydride. *Tappi, 47*, 557–564.
Zhang, J., Feng, X., Wang, J., Fang, G., Liu, J., & Wang, S. (2020). Nano-crystalline cellulose-coated magnetic nanoparticles for affinity adsorption of glycoproteins. *Analyst, 145*(9), 3407–3413.
Zhang, L., Ge, H., Xu, M., Cao, J., & Dai, Y. (2017). Physicochemical properties, antioxidant and antibacterial activities of dialdehyde microcrystalline cellulose. *Cellulose, 24*(5), 2287–2298.
Zhang, S., Kai, C., Liu, B., Zhang, S., Wei, W., Xu, X., et al. (2019). Preparation, characterization and antibacterial properties of cellulose membrane containing N-halamine. *Cellulose, 26*(9), 5621–5633.
Zhang, H., Liu, P., Peng, X., Chen, S., & Zhang, K. (2019). Interfacial synthesis of cellulose-derived solvent-responsive nanoparticles via Schiff base reaction. *ACS Sustainable Chemistry & Engineering, 7*(19), 16595–16603.
Zhang, H., Liu, P., Musa, S. M., Mai, C., & Zhang, K. (2019). Dialdehyde cellulose as a bio-based robust adhesive for wood bonding. *ACS Sustainable Chemistry & Engineering, 7*(12), 10452–10459.
Zheng, X., Li, X., Li, J., Wang, L., Jin, W., Pei, Y., et al. (2018). Efficient removal of anionic dye (Congo red) by dialdehyde microfibrillated cellulose/chitosan composite film with significantly improved stability in dye solution. *International Journal of Biological Macromolecules, 107*, 283–289.
Zhou, M., Hintermair, U., Hashiguchi, B. G., Parent, A. R., Hashmi, S. M., Elimelech, M., et al. (2013). Cp* iridium precatalysts for selective C–H oxidation with sodium periodate as the terminal oxidant. *Organometallics, 32*(4), 957–965.